DEUTSCHES ELEKTRONEN-SYNCHROTRON **DESY**

DESY 74/45
September 1974

Production of Hyperons by Virtual Photons

by

T. Azemoon, I. Dammann, C. Driver, D. Lüke, G. Specht
Deutsches Elektronen-Synchrotron DESY, Hamburg

K. Heinloth
Universität Bonn

H. Ackermann, E. Ganßauge
Universität Marburg

F. Janata, D. Schmidt
Bergische Universität
Gesamthochschule Wuppertal

2 HAMBURG 52 · NOTKESTIEG 1

To be sure that your preprints are promptly included in the
HIGH ENERGY PHYSICS INDEX ,
send them to the following address (if possible by air mail) :

DESY
Bibliothek
2 Hamburg 52
Notkestieg 1
Germany

PRODUCTION OF HYPERONS BY VIRTUAL PHOTONS

T. Azemoon, I. Dammann, C. Driver,
D. Lüke, G. Specht
Deutsches Elektronen-Synchrotron DESY

K. Heinloth
Universität Bonn

H. Ackermann, E. Ganßauge
Universität Marburg

F. Janata, D. Schmidt
Bergische Universität
Gesamthochschule Wuppertal

Abstract

The electroproduction of K^+Y on protons,

$$e\ p \rightarrow e\ K^+\ Y \qquad (Y \equiv \Lambda;\ \Sigma^o;\ \Sigma'^o(1385),\ \Lambda'(1405);\ \Lambda'(1520))$$

was investigated by measuring the scattered electron and the produced K^+-meson in coincidence. The differential cross sections were determined as functions of W, q^2, t and $\phi_{K\gamma}$ in the kinematical region:

$$1.9 \leq W \leq 2.8 \qquad \text{GeV}$$

$$-0.10 \geq q^2 \geq -0.60 \qquad \text{GeV}^2/c^2$$

$$t_{min} \geq t \geq t_{min}-0.33 \qquad \text{GeV}^2/c^2$$

$$0 \leq \phi_{K\gamma} \leq 360^o$$

Introduction

We present data on the hyperon production on protons by virtual photons via

$$e\,p \rightarrow e\,K^{+}\,Y\,; \qquad Y \equiv \Lambda;\ \Sigma^{o};\Sigma'^{o}(1385),\ \Lambda'(1405);\ \Lambda'(1520).$$

By detecting coincidences between the scattered electron and the produced K^{+}-meson the cross sections have been measured as functions of the following variables:

the four-momentum squares

of the $(\gamma_v p)$ system $\quad W^2 = (\gamma_v + p)^2$,

of the virtual photon $\quad q^2 = (e - e')^2$,

of all unobserved hadrons in the final state $\quad M^2 = (\gamma_v + p - K)^2$,

the square of the four-momentum transfer to the hyperon $\quad t = (p - Y)^2$,

(or equivalently $\quad t' = t - t_{min}$,

where t_{min} = minimum four-momentum transfer t at fixed values of q^2 and W),

and the azimuthal angle $\phi_{K\gamma}$, which is the angle between the polarization plane, subtended by $\vec{e}$ and $\vec{e}'$, and the production plane, subtended by $\vec{K}$ and the hyperon $\vec{Y}$ as defined in Fig. 1.

e, e', γ_v, K, p, Y are the four-momenta of the participating particles: the primary and the scattered lepton, the virtual photon, the K-meson, the target proton and the produced hyperon.

Results have been obtained in the following kinematical region:

$$1.9 \leq W \leq 2.8 \qquad \text{GeV},$$

$$-0.10 \geq q^2 \geq -0.60 \qquad \text{GeV}^2/c^2,$$

$$t_{min} \geq t \geq t_{min} - 0.33 \qquad \text{GeV}^2/c^2,$$

$$0 \leq \phi_{K\gamma} \leq 360^{o}.$$

The transverse photon polarization

$$\varepsilon = \left[1 + 2\,\frac{\vec{q}^{\,2}}{|q^2|}\,tg^2\,\frac{\theta_{ee'}}{2}\right]^{-1}$$

varied in the range $0.5 \leq \varepsilon \leq 0.8$.

Assuming the validity of the one-photon exchange the general form of the differential cross section for the electroproduction of hadrons can be written as[1]:

$$\frac{d^4\sigma}{dW^2\ dq^2\ dt\ d\phi_{K\gamma}} = \Gamma \times \left\{ \frac{d\sigma_u}{dt}(W,q^2,t) + \varepsilon \frac{d\sigma_L}{dt}(W,q^2,t) + \right.$$

$$\left. + \varepsilon \frac{d\sigma_P}{dt}(W,q^2,t) \cos 2\phi_{K\gamma} + \sqrt{2\varepsilon(\varepsilon+1)} \frac{d\sigma_I}{dt}(W,q^2,t) \cos\phi_{K\gamma} \right\} \qquad (1)$$

with

$$\Gamma = \frac{\alpha}{4(2\pi)^2} \cdot \frac{1}{E_e^2 \cdot M_p^2 \cdot |q^2|} \cdot \frac{W^2 - M_p^2}{1 - \varepsilon} \quad .$$

The cross section is separated into parts due to the two transverse and the longitudinal components of the virtual photon polarization. $d\sigma_u/dt$ is the differential cross section for unpolarized transverse virtual photons. It can, therefore, also be written as half the sum of the two cross sections $d\sigma_{||}/dt$ and $d\sigma_{\perp}/dt$ for transverse photons being polarized parallel and perpendicular to the production plane. In the limit $q^2 \to 0$ it has to approach the cross section for unpolarized real photons. The term $\varepsilon \cdot d\sigma_P/dt \cdot \cos 2\phi_{K\gamma}$ is the contribution of the transverse linear polarization to the cross section. $d\sigma_P/dt$ is half the difference between the two cross sections $d\sigma_{||}/dt$ and $d\sigma_{\perp}/dt$. $d\sigma_L/dt$ is the differential cross section for production with longitudinal photons. The term $\sqrt{2\ \varepsilon(\varepsilon+1)} \cdot d\sigma_I/dt \cdot \cos\phi_{K\gamma}$ takes account of the interference between the transverse and longitudinal components $d\sigma_{||}/dt$ and $d\sigma_L/dt$ of the virtual photon polarization.

By measuring the azimuthal dependence of the cross section we have separated the components $d\sigma_u/dt + \varepsilon\, d\sigma_L/dt$, $d\sigma_P/dt$ and $d\sigma_I/dt$ and have determined their dependence on W, q^2 and t (or equivalently t').

Apparatus

The layout of the apparatus is sketched in Fig. 2. The scattered electron and the produced K-meson were detected in coincidence in two spark-chamber spectrometers. After deflection by a magnetic field both particles were detected in optical spark chambers. The electron was identified by means of a Čerenkov and a shower counter. The K-mesons were identified by measuring the difference between the time-of-flight of the hadron and that of the electron. This was achieved by placing two scintillation hodoscopes in the rear of the two spectrometer arms. Pions with momenta above 1.8 GeV/c were vetoed by a threshold Čerenkov counter. The spark chamber tracks and all counter information were photographed and the pictures were analyzed automatically.

Measurement and Data Analysis

A total number of 600 000 pictures were taken for the reactions

$$e\,p \rightarrow e \begin{Bmatrix} K^+ \\ \pi^+ \\ p \end{Bmatrix} + \text{(additional hadrons)}$$

at primary electron energies of 4.0 and 4.9 GeV, which cover two different q^2-regions.

Figs. 3a and 3b depict two typical mass spectra for hadrons in momentum intervals below and above the pion threshold of the Čerenkov counter (p_π = 1.8 GeV/c). The mass was calculated using the measured path length, the momentum and the time-of-flight of the particle. For further analysis of K-production, only events under the K-peak were used after applying proper cuts[6].

To separate the different channels the missing mass M, defined by

$$M^2 = (\gamma_v + p - K)^2$$

was studied. As an example, the missing mass spectrum obtained for a primary energy of 4.9 GeV is shown in Fig. 4. Pronounced signals around the masses of 1.12 GeV/c^2 (Λ), 1.19 GeV/c^2 (Σ^0), 1.40 GeV/c^2 (Σ'^0(1385),Λ'(1405), which cannot be separated) and 1.52 GeV/c^2 (Λ'(1520)) show up above the background. The mass spectra, weighted with the acceptance of the apparatus, were fitted with Gaussian distri-

butions for Λ, Σ^o and $\Lambda'(1520)$ and with a single Breit-Wigner distribution for $\Sigma'^o(1385)$, $\Lambda'(1405)$ pair. A polynomial took account of the background which at the lower missing mass region was mainly due to pion production where the pion was misidentified as a kaon. Moreover each Gaussian distribution was distorted with a radiative tail to higher masses, whose shape was parametrized in such a way that the area under the tail corresponded to the calculated value of the radiative corrections[2] (10 - 20 %). Typical mass spectra are given in Fig. 5a for Λ and Σ^o and in Fig. 5b for the resonance states.

The following ranges in the mass spectra were used to identify the different channels:

Λ	1.03 - 1.16 GeV/c^2
Σ^o	1.16 - 1.25 GeV/c^2
$\Sigma'^o(1385)$, $\Lambda'(1405)$	1.35 - 1.45 GeV/c^2
$\Lambda'(1520)$	1.49 - 1.55 GeV/c^2

The cross sections were corrected for the losses due to the cuts in the missing mass (< 5 % for Gaussian, 40 % for Breit-Wigner), for the background (20 - 50 % depending on the reaction), for the efficiency loss in the trigger, Čerenkov and shower counters (6 %), for the interaction of the K-mesons (6 %), for the decay of the K-mesons (50 - 70 % depending on the momentum), for loss of events by the automatic data analysis procedure (10 %), and for the loss of events due to the cuts in the time-of-flight spectra (5 - 60 % depending on the momentum). The uncertainties in all these corrections including that in the intensity of the primary beam add up to an overall systematic error of about ±10 %. The uncertainty in the fraction of the hyperon contributions in the missing mass fits causes uncertainties in the cross sections of ±5 % for Λ, ±12 % for Σ^o, ±10 % for $\Sigma'^o(1385)$, $\Lambda'(1405)$ and ±10 % for $\Lambda'(1520)$.

Results

The cross sections $d\sigma_u/dt + \varepsilon\, d\sigma_L/dt$, $d\sigma_P/dt$ and $d\sigma_I/dt$, defined in Eq. (1), are given as functions of W, t and q^2 in tables 1 - 4 and Figs. 6 - 15. The cross sections for all reactions are dominated by the sum of the unpolarized transverse and the longitudinal cross section $d\sigma_u/dt + \varepsilon\, d\sigma_L/dt$. The absolute values

of the cross sections $d\sigma_p/dt$ and $d\sigma_I/dt$ are of the order of 10 % of $d\sigma_u/dt + \varepsilon\, d\sigma_L/dt$ and within their error bars they are compatible with zero (Figs. 6, 7, 14 and 15).

For a part of the accepted kinematical region the data covered the $\phi_{K\gamma}$ interval between -60° and 60°, in which case the cross sections were averaged over this interval. Their values are also given in tables 1 – 4 under $d\sigma_u/dt + \varepsilon\, d\sigma_L/dt$. As the measured values of $d\sigma_I/dt$ and $d\sigma_p/dt$ for the neighbouring kinematical region are compatible with zero, it can be assumed that the same result also holds for the above region, so that the averaged cross section is roughly equal to $d\sigma_u/dt + \varepsilon\, d\sigma_L/dt$.

These results replace the preliminary values for $K^+\Lambda$ amd $K^+\Sigma^o$ cross sections of this experiments presented at the International Symposium on Electron and Photon Interactions at High Energies, Bonn[9]. In the earlier version a wrong number of incoming electrons was used in the data analysis.

W-Dependence of the Cross Sections for $K^+\Lambda$ and $K^+\Sigma^o$

The W-dependence of the cross sections is shown in Fig. 8 ($K^+\Lambda$) and Fig. 9 ($K^+\Sigma^o$). In the range $2.15 < W < 2.35$ GeV and for relatively low values of $|q^2|$ the cross section $d\sigma_u/dt + \varepsilon\, d\sigma_L/dt$ exhibits a very strong dependence on W. In this region its behaviour is compatible with $(W^2 - M_p^2)^{-3.5\pm.3}$ for $K^+\Lambda$ and with $(W^2 - M_p^2)^{-2.9\pm.3}$ for $K^+\Sigma^o$. At higher values of W and $|q^2|$ the W-dependence becomes weaker and the data for $K^+\Lambda$ and $K^+\Sigma^o$ can be described by $(W^2 - M_p^2)^{-2.4\pm.2}$ and $(W^2 - M_p^2)^{-2.2\pm.2}$ respectively. It should be noted that the kinematical points with lower values of W, keeping the other variables fixed, correspond to higher values of ε. Therefore a non-vanishing $d\sigma_L/dt$ would result in a varying normalization of $d\sigma_u/dt + \varepsilon\, d\sigma_L/dt$ along the W-axis, and hence in a steeper W-dependence. For the present data the effect is of the order of 10 % in the exponent.

One possible explanation for the observed variation of the W-dependence of the cross section $d\sigma_u/dt + \varepsilon\, d\sigma_L/dt$ could be that $d\sigma_u/dt$ and $d\sigma_L/dt$ depend differently on W. With increasing $|q^2|$ the relative contribution of the two components can vary and produce the above effect.

t-Dependence of the Cross Sections for $K^+\Lambda$ and $K^+\Sigma^o$

Figs. 10 and 11 show the t-dependence of the cross section $d\sigma_u/dt + \varepsilon\, d\sigma_L/dt$ for $K^+\Lambda$ and $K^+\Sigma^o$ respectively. As it can be seen, the dependence of this cross section on t is rather weak.

q^2-Dependence of the Cross Sections

The q^2-dependence of $d\sigma_u/dt + \varepsilon\, d\sigma_L/dt$ is shown in Figs. 12 - 15 where our data are plotted together with the photoproduction data[3,8]. For this purpose part of the data were extrapolated in W according to the proper dependences indicated in the relevant figures. The data for $K^+\Lambda$ and $K^+\Sigma^o$ have been obtained at slightly different values of t, all close to $t = -.15\ GeV^2/c^2$. No extrapolation in t was applied to the data since the electroproduction cross sections for $K^+\Lambda$ and $K^+\Sigma^o$ vary only slightly around this t-value. For all the four channels the cross section $d\sigma_u/dt + \varepsilon\, d\sigma_L/dt$ decreases smoothly with increasing $|q^2|$, starting from the photoproduction point at $q^2 = 0$. The behaviour of the above cross section for all channels except for $K^+\Lambda$ is compatible with the predictions of a simple Vector-Meson Dominance Model for $d\sigma_u/dt$. In the case of $K^+\Lambda$ the cross section falls less rapidly even compared to the total transverse cross section normalized to the photoproduction value. This may be due to a large contribution of the longitudinal component which can be explained by a K-exchange in the t-channel, in analogy with the electroproduction of π^+n where the remarkably large contribution of the longitudinal part was also attributed to the exchange of a pseudoscalar meson in the t-channel (pion exchange). If this explanation is correct one would expect a much smaller longitudinal part in the case of $K^+\Sigma^o$ due to the difference in the coupling constants

$$g^2_{K\Lambda N} \gg g^2_{K\Sigma N},$$

in agreement with the observed behaviour of the cross section for $K^+\Sigma^o$ (Fig. 13). On the other hand a large contribution from the longitudinal part in the case of $K^+\Lambda$ would be in disagreement with a theoretical prediction[7] based on a Regge Model.

The cross sections for $K^+\Lambda$ obtained in the present experiment lie about 25 % below the other published values[4,5]. This could be explained by the larger values of ε in the above references together with the existence of a large longitudinal component.

Acknowledgements

Some of us (H. Ackermann, E. Ganßauge, F. Janata, D. Schmidt) would like to thank Professors H. Schopper and G. Weber for the kind hospitality at DESY. We also want to thank Mr. G. Augustinski, Mr. P. Burmeister, Mr. K. Maschidlauskas, Mrs. B. Nissen and Mrs. R. Siemer for their excellent assistance. The valuable cooperation of the Synchrotron crew, the Hallendienst, the Kältetechnik and the Rechenzentrum is gratefully acknowledged.

Literature

1) L.N. Hand; Phys. Rev. 129, 1834 (1963)
S.M. Berman; Phys. Rev. 135,1249 (1964)

2) C. de Calan, G. Fuchs; Nuovo Cim. 38, 1594 (1965) and
Nuovo Cim. 41, 286 (1966)

3) P. Feller et al.; Nucl. Phys. B39, 413 (1972)

4) C.N. Brown et al.; Phys. Rev. Lett. 28, 1086 (1972)

5) C.J. Bebek et al.; Phys. Rev. Lett. 32, 21 (1974)

6) F. Janata; Thesis, Hamburg (1974) (to be published)

7) N. Levy et al.; Nucl. Phys. B55, 493 and 513 (1973)

8) H. Burfeindt et al.; Contribution to the International Symposium
on Electron and Photon Interactions at High Energies, Bonn, August 1973

9. T. Azemoon et al.; Contribution to the International Symposium on
Electron and Photon Interactions at High Energies, Bonn August 1973,
Abstract No. 73

Figure Captions

1) Diagram of the reaction $e\,p \rightarrow e\,K^+\,Y$.

2) Experimental layout.

3) Spectrum of m_h^2 (calculated using the time-of-flight information) of the detected hadrons for the momentum interval

   a) $1.2 \leq |\vec{p}_h| \leq 1.25$ GeV/c,

   b) $2.05 \leq |\vec{p}_h| \leq 2.1$ GeV/c.

4) Spectrum of the missing mass $M = \sqrt{(\gamma_v + p - K)^2}$ for the reaction $\gamma_v\,p \rightarrow K^+ +$(additional hadrons) obtained with a primary electron energy of 4.9 GeV.

5) Missing mass distributions obtained in the kinematical regions

   a) $-0.42 \leq q^2 \leq -0.20$ GeV^2/c^2,
   $1.95 \leq W \leq 2.25$ GeV,
   $-0.20 \leq t \leq -0.054$ GeV^2/c^2,
   $0 \leq \phi_{K\gamma} \leq 360^\circ$;

   b) $-0.60 \leq q^2 \leq -0.10$ GeV^2/c^2,
   $2.10 \leq W \leq 2.80$ GeV,
   $-0.35 \leq t' \leq 0.0$ GeV^2/c^2,
   $0 \leq \phi_{K\gamma} \leq 360^\circ$.

6) The dependence of the cross sections $d\sigma_u/dt + \varepsilon d\sigma_L/dt$, $d\sigma_I/dt$ and $d\sigma_P/dt$ on W, q^2 and t for $\gamma_v p \rightarrow K^+\Lambda$, obtained with a primary electron energy of

   a) 4.0 GeV,

   b) 4.9 GeV.

7) The dependence of the cross sections $d\sigma_u/dt + \varepsilon\, d\sigma_L/dt$, $d\sigma_I/dt$ and $d\sigma_P/dt$ on W, q^2 and t for $\gamma_v p \rightarrow K^+\Sigma^0$, obtained with a primary electron energy of

   a) 4.0 GeV,

   b) 4.9 GeV.

8) W-dependence of $d\sigma_u/dt + \varepsilon\, d\sigma_L/dt$ for $\gamma_v p \to K^+\Lambda$ in two different kinematical regions.

9) W-dependence of $d\sigma_u/dt + \varepsilon\, d\sigma_L/dt$ for $\gamma_v p \to K^+\Sigma^o$ in two different kinematical regions.

10) t-dependence of $d\sigma_u/dt + \varepsilon\, d\sigma_L/dt$ for $\gamma_v p \to K^+\Lambda$ in two different kinematical regions.

11) t-dependence of $d\sigma_u/dt + \varepsilon\, d\sigma_L/dt$ for $\gamma_v p \to K^+\Sigma^o$ in two different kinematical regions.

12) q^2-dependence of $d\sigma_u/dt + \varepsilon\, d\sigma_L/dt$ for $\gamma_v p \to K^+\Lambda$. For comparison the curves corresponding to the total transverse cross section and a simple VDM prediction, both normalized to the photoproduction value, are given.

13) q^2-dependence of $d\sigma_u/dt + \varepsilon\, d\sigma_L/dt$ for $\gamma_v p \to K^+\Sigma^o$. For comparison the curves corresponding to the total transverse cross section and a simple VDM prediction, both normalized to the photoproduction value, are given.

14) q^2-dependence of $d\sigma_u/dt + \varepsilon\, d\sigma_L/dt$, $d\sigma_I/dt$ and $d\sigma_p/dt$ for $\gamma_v p \to K^+\Sigma'^o(1385),\Lambda'(1405)$. For comparison the curve corresponding to a simple VDM prediction, normalized to the photoproduction value, is given. This photoproduction value is obtained by extrapolating with $(W^2-M_p^2)^{-2}$.

15) q^2-dependence of $d\sigma_u/dt + \varepsilon\, d\sigma_L dt$, $d\sigma_I/dt$ and $d\sigma_p/dt$ for $\gamma_v p \to K^+\Lambda'(1520)$. For comparison the curve corresponding to a simple VDM prediction, normalized to the photoproduction value, is given. This photoproduction value is obtained by extrapolating with $(W^2-M_p^2)^{-2}$.

Table 1a W-dependence of the cross sections

$$\frac{d\sigma_u}{dt} + \varepsilon \frac{d\sigma_L}{dt}, \quad \frac{d\sigma_I}{dt} \text{ and } \frac{d\sigma_P}{dt}$$

for $\gamma_v p \to K^+ \Lambda$

W	$\lvert q^2 \rvert$	$\lvert t \rvert$	ε	$\frac{d\sigma_u}{dt} + \varepsilon \frac{d\sigma_L}{dt}$	$\frac{d\sigma_I}{dt}$	$\frac{d\sigma_P}{dt}$
2.00 - 2.10	.22 - .42	.06 - .17	.80	2.27 ±.22	-.23 ±.20	-.49 ±.40
2.10 - 2.20	.22 - .42	.06 - .17	.74	1.84 ±.18	-.16 ±.17	.14 ±.28
2.00 - 2.16	.21 - .33	.06 - .15	.79	2.11 ±.28	-	-
2.16 - 2.21	.16 - .39	.05 - .17	.73	1.68 ±.16	-	-
2.21 - 2.24	.17 - .37	.05 - .17	.70	1.35 ±.18	-	-
2.24 - 2.36	.22 - .32	.06 - .16	.65	.88 ±.10	-	-
2.10 - 2.22	.46 - .60	.08 - .22	.81	1.18 ±.17	-.20 ±.16	.36 ±.25
2.22 - 2.34	.46 - .60	.08 - .22	.76	.84 ±.09	-.06 ±.08	-.08 ±.18
2.28 - 2.40	.31 - .49	.07 - .20	.74	.86 ±.08	-	-
2.40 - 2.44	.29 - .51	.07 - .20	.70	.84 ±.10	-	-
2.44 - 2.48	.31 - .49	.07 - .20	.67	.64 ±.10	-	-
2.48 - 2.60	.34 - .46	.07 - .20	.61	.53 ±.09	-	-

Units:

W in GeV

q^2, t in GeV^2/c^2

cross sections in $\mu b\ GeV^{-2}c^2$

Table 1b t-dependence of the cross sections

$$\frac{d\sigma_u}{dt} + \varepsilon \frac{d\sigma_L}{dt}, \quad \frac{d\sigma_I}{dt} \text{ and } \frac{d\sigma_P}{dt}$$

for $\gamma_v p \rightarrow K^+ \Lambda$

W	$\lvert q^2 \rvert$	$\lvert t \rvert$	ε	$\frac{d\sigma_u}{dt} + \varepsilon \frac{d\sigma_L}{dt}$	$\frac{d\sigma_I}{dt}$	$\frac{d\sigma_P}{dt}$
2.00 - 2.20	.22 - .42	.06 - .11	.74	1.84 ±.15	.19 ±.13	-.31 ±.29
2.00 - 2.20	.22 - .42	.11 - .17	.77	1.82 ±.20	-.18 ±.20	.22 ±.36
2.12 - 2.40	.11 - .29	.06 - .08	.69	1.15 ±.10	-	-
2.08 - 2.44	.12 - .28	.08 - .10	.69	1.17 ±.10	-	-
2.12 - 2.44	.13 - .27	.10 - .12	.68	1.14 ±.11	-	-
2.16 - 2.44	.12 - .28	.12 - .14	.66	1.12 ±.12	-	-
2.20 - 2.48	.14 - .26	.14 - .17	.63	.85 ±.11	-	-
2.10 - 2.34	.46 - .60	.08 - .14	.79	.99 ±.09	-.05 ±.09	.35 ±.18
2.10 - 2.34	.46 - .60	.14 - .22	.79	.96 ±.33	-.15 ±.33	-.17 ±.47
2.24 - 2.52	.30 - .50	.07 - .10	.72	.85 ±.10	-	-
2.24 - 2.52	.30 - .50	.10 - .12	.71	.91 ±.10	-	-
2.28 - 2.60	.29 - .51	.12 - .14	.70	.61 ±.09	-	-
2.36 - 2.68	.20 - .40	.14 - .16	.66	.62 ±.09	-	-
2.36 - 2.64	.20 - .40	.16 - .18	.64	.57 ±.08	-	-
2.40 - 2.72	.20 - .40	.18 - .20	.63	.55 ±.08	-	-

Units:

W in GeV

q^2, t in GeV^2/c^2

cross sections in $\mu b\ GeV^{-2}c^2$

Table 1c q^2-dependence of the cross sections

$$\frac{d\sigma_u}{dt} + \varepsilon \frac{d\sigma_L}{dt}, \quad \frac{d\sigma_I}{dt} \text{ and } \frac{d\sigma_P}{dt}$$

for $\gamma_v p \to K^+\Lambda$

W	$\lvert q^2 \rvert$	$\lvert t \rvert$	ε	$\frac{d\sigma_u}{dt} + \varepsilon \frac{d\sigma_L}{dt}$	$\frac{d\sigma_I}{dt}$	$\frac{d\sigma_P}{dt}$
2.00 - 2.20	.22 - .32	.06 - .17	.78	2.12 ±.16	.09 ±.14	-.36 ±.28
2.00 - 2.20	.32 - .42	.06 - .17	.76	1.84 ±.18	-.09 ±.17	.15 ±.34
2.12 - 2.48	.10 - .15	.05 - .17	.68	.91 ±.08	-	-
2.10 - 2.48	.15 - .20	.06 - .16	.68	1.13 ±.08	-	-
2.08 - 2.40	.20 - .25	.06 - .16	.70	1.29 ±.10	-	-
2.04 - 2.36	.25 - .34	.07 - .15	.72	1.43 ±.13	-	-
2.10 - 2.34	.46 - .53	.08 - .22	.77	.99 ±.09	-.05 ±.09	.35 ±.18
2.10 - 2.34	.53 - .60	.08 - .22	.77	.96 ±.33	-.15 ±.33	-.17 ±.47
2.48 - 2.76	.15 - .20	.17 - .33	.59	.31 ±.04	-	-
2.48 - 2.76	.20 - .25	.17 - .33	.58	.43 ±.05	-	-
2.36 - 2.64	.25 - .31	.06 - .22	.66	.61 ±.06	-	-
2.32 - 2.64	.31 - .36	.08 - .20	.67	.71 ±.08	-	-
2.24 - 2.60	.36 - .41	.07 - .21	.70	.78 ±.08	-	-
2.20 - 2.60	.41 - .48	.08 - .20	.70	.74 ±.08	-	-

Units:

W in GeV

q^2, t in GeV^2/c^2

cross sections in $\mu b\ GeV^{-2}c^2$

Table 2a W-dependence of the cross sections

$$\frac{d\sigma_u}{dt} + \varepsilon \frac{d\sigma_L}{dt}, \quad \frac{d\sigma_I}{dt} \text{ and } \frac{d\sigma_P}{dt}$$

for $\gamma_v p \to K^+\Sigma^o$

W	$\lvert q^2 \rvert$	$\lvert t \rvert$	ε	$\frac{d\sigma_u}{dt} + \varepsilon \frac{d\sigma_L}{dt}$	$\frac{d\sigma_I}{dt}$	$\frac{d\sigma_P}{dt}$
2.00 - 2.10	.22 - .40	.10 - .20	.80	1.09 ±.16	.06 ±.14	-.02 ±.24
2.10 - 2.20	.22 - .40	.10 - .20	.75	.42 ±.08	.03 ±.08	-.13 ±.14
2.08 - 2.20	.16 - .28	.08 - .20	.77	.61 ±.09	-	-
2.20 - 2.26	.12 - .32	.08 - .20	.71	.53 ±.05	-	-
2.26 - 2.30	.11 - .33	.08 - .20	.67	.37 ±.05	-	-
2.30 - 2.40	.13 - .31	.08 - .20	.62	.34 ±.07	-	-
2.10 - 2.22	.46 - .60	.12 - .24	.81	.31 ±.13	-.04 ±.13	-.12 ±.16
2.22 - 2.34	.46 - .60	.12 - .24	.76	.25 ±.04	-.01 ±.04	.02 ±.08
2.36 - 2.48	.24 - .38	.10 - .20	.70	.24 ±.03	-	-
2.48 - 2.52	.21 - .41	.10 - .20	.66	.25 ±.04	-	-
2.52 - 2.56	.18 - .44	.10 - .20	.64	.25 ±.04	-	-
2.56 - 2.68	.22 - .44	.10 - .20	.58	.15 ±.03	-	-

Units:

W in GeV

q^2, t in GeV^2/c^2

cross sections in $\mu b\ GeV^{-2}c^2$

Table 2b t-dependence of the cross sections

$$\frac{d\sigma_u}{dt} + \varepsilon \frac{d\sigma_L}{dt}, \quad \frac{d\sigma_I}{dt}, \quad \text{and} \quad \frac{d\sigma_P}{dt}$$

for $\gamma_v p \rightarrow K^+ \Sigma^o$

W	$\lvert q^2 \rvert$	$\lvert t \rvert$	ε	$\frac{d\sigma_u}{dt} + \varepsilon \frac{d\sigma_L}{dt}$	$\frac{d\sigma_I}{dt}$	$\frac{d\sigma_P}{dt}$
2.00 - 2.20	.22 - .40	.10 - .15	.78	.62 ±.08	-.04 ±.07	-.03 ±.13
2.00 - 2.20	.22 - .40	.15 - .20	.78	1.06 ±.24	.21 ±.23	.12 ±.34
2.16 - 2.40	.11 - .27	.08 - .10	.68	.39 ±.05	-	-
2.08 - 2.44	.12 - .26	.10 - .12	.70	.41 ±.05	-	-
2.08 - 2.48	.10 - .28	.12 - .14	.68	.45 ±.05	-	-
2.16 - 2.48	.12 - .26	.14 - .17	.65	.48 ±.05	-	-
2.24 - 2.44	.11 - .27	.17 - .20	.63	.28 ±.05	-	-
2.10 - 2.34	.46 - .60	.12 - .18	.79	.28 ±.04	.02 ±.04	-.04 ±.08
2.10 - 2.34	.46 - .60	.18 - .24	.79	.22 ±.16	-.09 ±.16	-.10 ±.21
2.28 - 2.52	.22 - .44	.10 - .12	.71	.28 ±.05	-	-
2.28 - 2.56	.24 - .42	.12 - .14	.70	.25 ±.04	-	-
2.36 - 2.64	.21 - .45	.14 - .16	.65	.22 ±.04	-	-
2.32 - 2.64	.18 - .48	.16 - .18	.67	.25 ±.04	-	-
2.40 - 2.68	.21 - .45	.18 - .20	.64	.19 ±.04	-	-

Units:

W in GeV

q^2, t in GeV^2/c^2

cross sections in $\mu b\ GeV^{-2}c^2$

Table 2c q^2-dependence of the cross sections

$$\frac{d\sigma_u}{dt} + \varepsilon \frac{d\sigma_L}{dt}, \quad \frac{d\sigma_I}{dt} \text{ and } \frac{d\sigma_P}{dt}$$

for $\gamma_v p \to K^+\Sigma^o$

W	$\lvert q^2 \rvert$	$\lvert t \rvert$	ε	$\frac{d\sigma_u}{dt} + \varepsilon \frac{d\sigma_L}{dt}$	$\frac{d\sigma_I}{dt}$	$\frac{d\sigma_P}{dt}$
2.00 - 2.20	.22 - .31	.10 - .20	.78	.76 ±.10	-.07 ±.09	-.06 ±.16
2.00 - 2.20	.31 - .40	.10 - .20	.77	.59 ±.09	-.02 ±.08	-.13 ±.17
2.20 - 2.52	.15 - .20	.07 - .21	.62	.30 ±.03	-	-
2.12 - 2.52	.20 - .24	.07 - .21	.64	.38 ±.04	-	-
2.08 - 2.44	.24 - .28	.09 - .19	.68	.37 ±.05	-	-
2.08 - 2.40	.28 - .36	.09 - .19	.68	.40 ±.07	-	-
2.10 - 2.34	.46 - .53	.12 - .24	.79	.29 ±.05	.02 ±.05	-.05 ±.10
2.10 - 2.34	.53 - .60	.12 - .24	.78	.24 ±.05	-.06 ±.05	-.07 ±.09
2.52 - 2.76	.15 - .21	.25 - .35	.57	.12 ±.02	-	-
2.40 - 2.68	.21 - .27	.10 - .24	.65	.25 ±.03	-	-
2.36 - 2.64	.27 - .33	.09 - .25	.66	.19 ±.02	-	-
2.28 - 2.64	.33 - .39	.10 - .24	.68	.23 ±.03	-	-
2.24 - 2.60	.39 - .49	.10 - .24	.71	.21 ±.03	-	-

Units:

W in GeV

q^2, t in GeV^2/c^2

cross sections in $\mu b\ GeV^{-2}c^2$

Table 3 cross sections $\frac{d\sigma_u}{dt} + \varepsilon \frac{d\sigma_L}{dt}$, $\frac{d\sigma_I}{dt}$ and $\frac{d\sigma_P}{dt}$

for $\gamma_v p \to K^+ \Sigma'^0(1385), \Lambda'(1405)$

W	$\lvert q^2 \rvert$	$\lvert t' \rvert$	ε	$\frac{d\sigma_u}{dt} + \varepsilon \frac{d\sigma_L}{dt}$	$\frac{d\sigma_I}{dt}$	$\frac{d\sigma_P}{dt}$
2.10 - 2.24	.23 - .37	.00 - .02	.73	1.67 ±.24	-.02 ±.24	.54 ±.47
2.24 - 2.38	.11 - .20	.00 - .10	.66	1.05 ±.08	-	-
2.24 - 2.38	.20 - .30	.00 - .10	.64	.90 ±.09	-	-
2.24 - 2.30	.11 - .30	.00 - .10	.68	1.22 ±.12	-	-
2.30 - 2.38	.11 - .30	.00 - .10	.63	.82 ±.07	-	-
2.24 - 2.38	.11 - .30	.00 - .04	.65	1.13 ±.10	-	-
2.24 - 2.38	.11 - .30	.04 - .10	.65	.86 ±.08	-	-
2.38 - 2.52	.09 - .13	.04 - .20	.55	.52 ±.05	-	-
2.38 - 2.52	.13 - .19	.04 - .20	.54	.56 ±.06	-	-
2.38 - 2.44	.09 - .19	.04 - .20	.58	.51 ±.05	-	-
2.44 - 2.52	.09 - .19	.04 - .20	.51	.58 ±.06	-	-
2.38 - 2.52	.09 - .19	.04 - .10	.54	.57 ±.06	-	-
2.38 - 2.52	.09 - .19	.10 - .20	.54	.52 ±.05	-	-
2.16 - 2.40	.40 - .50	.00 - .06	.77	.87 ±.09	-.02 ±.09	.20 ±.15
2.16 - 2.40	.50 - .60	.00 - .06	.75	.65 ±.08	.05 ±.07	.11 ±.18
2.16 - 2.28	.40 - .60	.00 - .06	.79	.86 ±.12	.09 ±.11	.05 ±.19
2.28 - 2.40	.40 - .60	.00 - .06	.73	.66 ±.08	.00 ±.08	.18 ±.15
2.16 - 2.40	.40 - .60	.00 - .02	.76	.86 ±.08	.02 ±.08	.08 ±.16
2.16 - 2.40	.40 - .60	.02 - .06	.76	.61 ±.09	.02 ±.09	.08 ±.16
2.40 - 2.60	.22 - .32	.02 - .18	.66	.43 ±.03	-	-
2.40 - 2.60	.32 - .44	.02 - .18	.65	.46 ±.04	-	-
2.40 - 2.50	.22 - .44	.02 - .18	.69	.51 ±.04	-	-
2.50 - 2.60	.22 - .44	.02 - .18	.62	.38 ±.03	-	-
2.40 - 2.60	.22 - .44	.02 - .08	.65	.45 ±.04	-	-
2.40 - 2.60	.22 - .44	.08 - .18	.65	.45 ±.04	-	-
2.60 - 2.76	.13 - .21	.13 - .33	.54	.29 ±.03	-	-
2.60 - 2.76	.21 - .31	.13 - .33	.52	.24 ±.03	-	-
2.60 - 2.68	.13 - .31	.13 - .33	.56	.29 ±.03	-	-
2.68 - 2.76	.13 - .31	.13 - .33	.49	.25 ±.03	-	-
2.60 - 2.76	.13 - .31	.13 - .21	.53	.32 ±.03	-	-
2.60 - 2.76	.13 - .31	.21 - .33	.53	.24 ±.03	-	-

Units: W in GeV; q^2, t' in GeV^2/c^2; cross sections in $\mu b\ GeV^{-2}c^2$

Table 4 Cross sections $\frac{d\sigma_u}{dt} + \varepsilon \frac{d\sigma_L}{dt}$, $\frac{d\sigma_I}{dt}$ and $\frac{d\sigma_P}{dt}$ for $\gamma_v p \to K^+\Lambda'(1520)$

W	$\lvert q^2 \rvert$	$\lvert t' \rvert$	ε	$\frac{d\sigma_u}{dt} + \varepsilon \frac{d\sigma_L}{dt}$	$\frac{d\sigma_I}{dt}$	$\frac{d\sigma_P}{dt}$
2.36 - 2.52	.08 - .12	.04 - .18	.56	.37 ±.05	-	-
2.36 - 2.52	.12 - .18	.04 - .18	.55	.42 ±.05	-	-
2.36 - 2.42	.08 - .18	.04 - .18	.60	.42 ±.07	-	-
2.42 - 2.52	.08 - .18	.04 - .18	.52	.38 ±.04	-	-
2.36 - 2.52	.08 - .18	.04 - .10	.56	.41 ±.05	-	-
2.36 - 2.52	.08 - .18	.10 - .18	.56	.41 ±.05	-	-
2.20 - 2.40	.12 - .20	.00 - .04	.67	.76 ±.10	-	-
2.20 - 2.40	.20 - .30	.00 - .04	.65	.54 ±.09	-	-
2.20 - 2.30	.12 - .30	.00 - .04	.70	.76 ±.11	-	-
2.30 - 2.40	.12 - .30	.00 - .04	.62	.56 ±.09	-	-
2.20 - 2.40	.12 - .30	.00 - .02	.66	.74 ±.10	-	-
2.20 - 2.40	.12 - .30	.02 - .04	.66	.58 ±.09	-	-
2.20 - 2.40	.35 - .45	.00 - .03	.77	.88 ±.16	-.14 ±.16	.23 ±.26
2.20 - 2.40	.45 - .55	.00 - .03	.75	.65 ±.10	-.07 ±.08	-.14 ±.16
2.20 - 2.32	.35 - .55	.00 - .03	.78	.82 ±.13	-.14 ±.11	-.23 ±.22
2.32 - 2.40	.35 - .55	.00 - .03	.72	.58 ±.17	.01 ±.18	.12 ±.25
2.20 - 2.40	.35 - .55	.00 - .01	.76	.77 ±.11	-.04 ±.09	-.28 ±.20
2.20 - 2.40	.35 - .55	.01 - .03	.76	.84 ±.15	-.18 ±.15	.40 ±.24
2.40 - 2.60	.22 - .34	.00 - .14	.66	.52 ±.03	-	-
2.40 - 2.60	.34 - .48	.00 - .14	.64	.37 ±.03	-	-
2.40 - 2.50	.22 - .48	.00 - .14	.69	.49 ±.04	-	-
2.50 - 2.60	.22 - .48	.00 - .14	.61	.41 ±.03	-	-
2.40 - 2.60	.22 - .48	.00 - .04	.65	.44 ±.04	-	-
2.40 - 2.60	.22 - .48	.04 - .08	.65	.50 ±.04	-	-
2.40 - 2.60	.22 - .48	.08 - .14	.65	.43 ±.04	-	-
2.60 - 2.80	.12 - .18	.10 - .30	.53	.17 ±.02	-	-
2.60 - 2.80	.18 - .30	.10 - .30	.51	.17 ±.02	-	-
2.60 - 2.70	.12 - .30	.10 - .30	.56	.20 ±.02	-	-
2.70 - 2.80	.12 - .30	.10 - .30	.47	.14 ±.02	-	-
2.60 - 2.80	.12 - .30	.10 - .20	.51	.17 ±.02	-	-
2.60 - 2.80	.12 - .30	.20 - .30	.51	.18 ±.02	-	-

Units: W in GeV; q^2, t' in GeV^2/c^2; cross sections in $\mu b\ GeV^{-2}c^2$

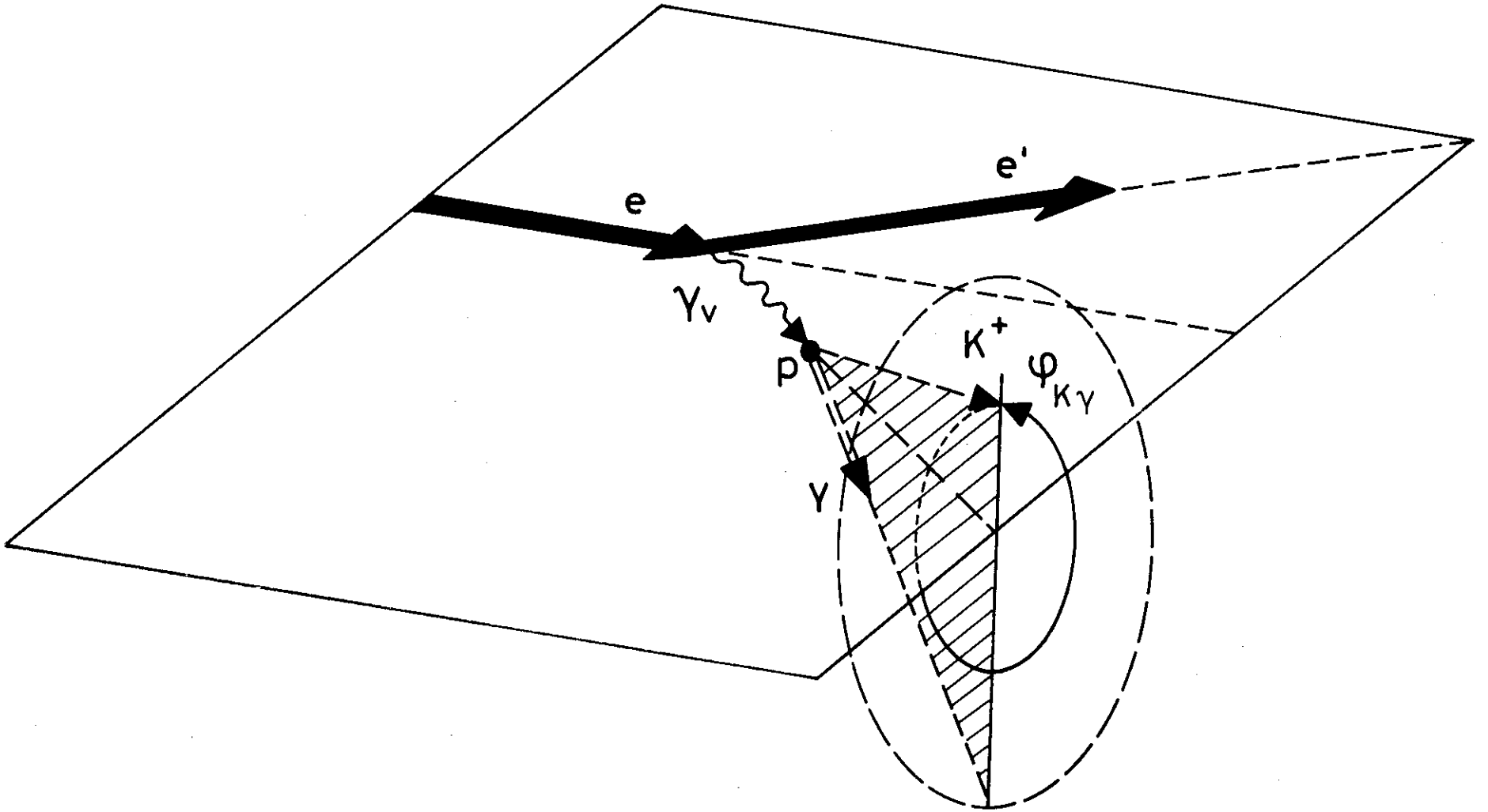

Fig. 1

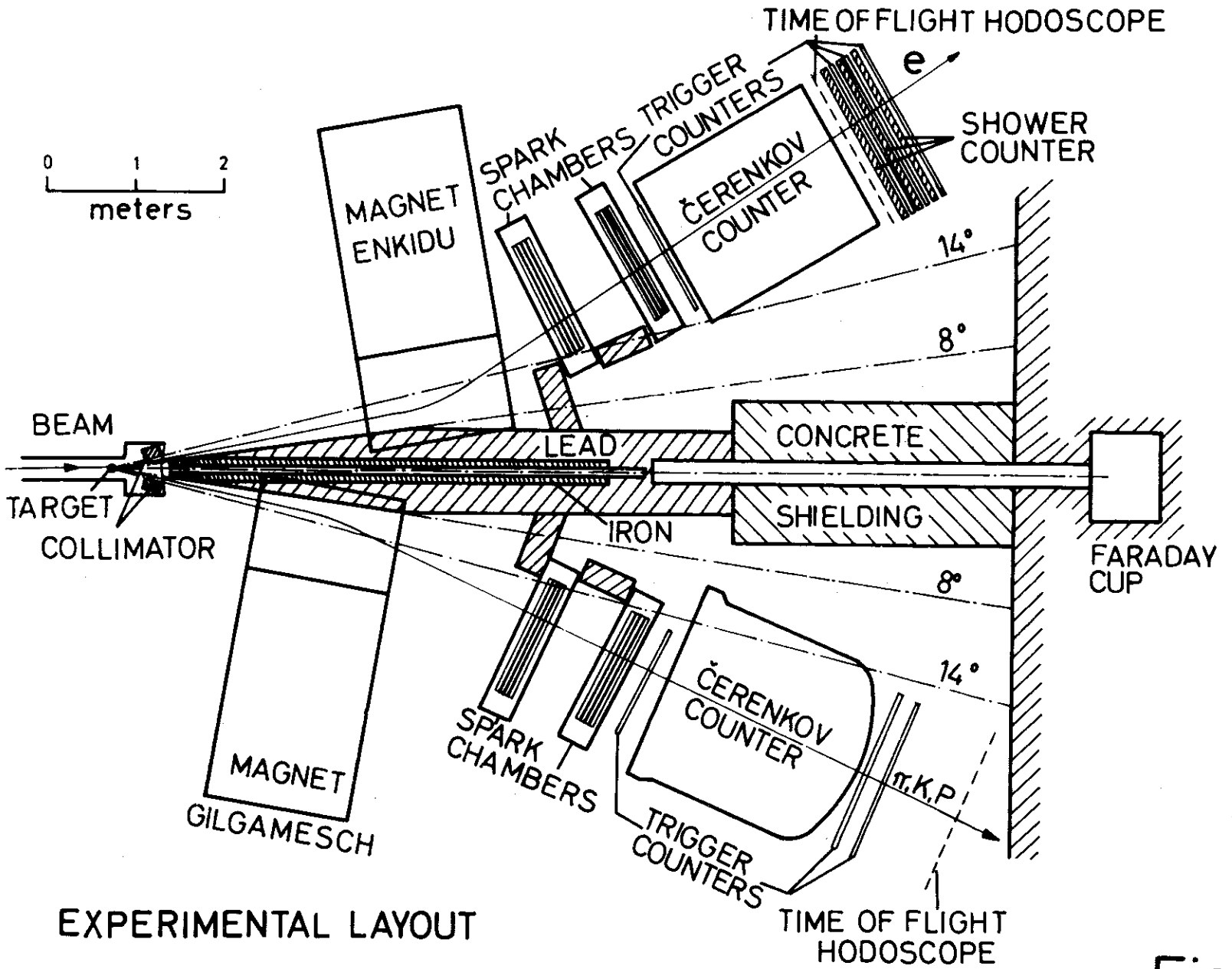

EXPERIMENTAL LAYOUT

Fig. 2

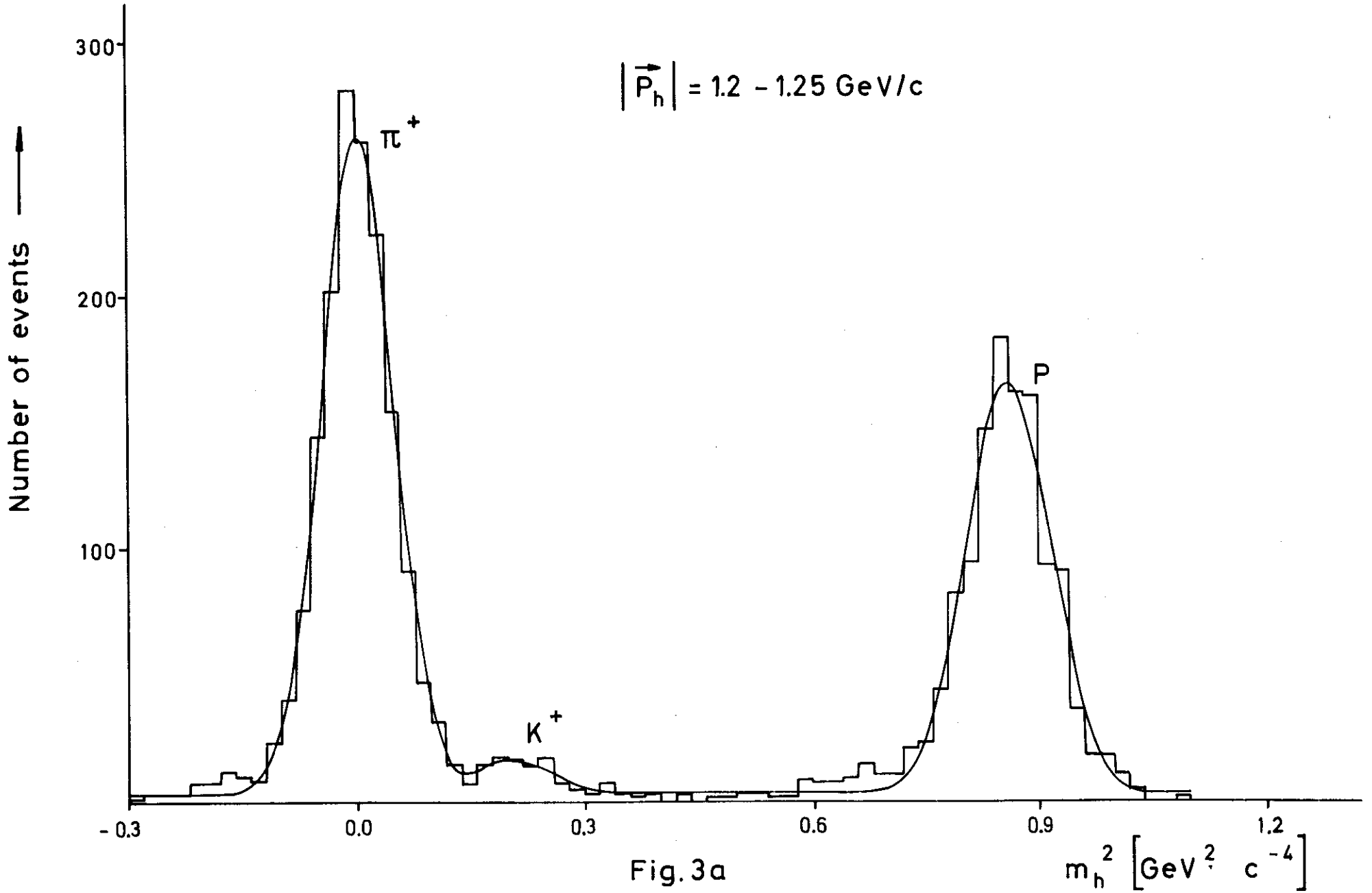
$|\vec{P}_h|$ = 1.2 - 1.25 GeV/c
Number of events
300
200
100
π^+
K^+
P
- 0.3
0.0
0.3
0.6
0.9
1.2
m_h^2 [GeV^2 c^{-4}]

Fig. 3a

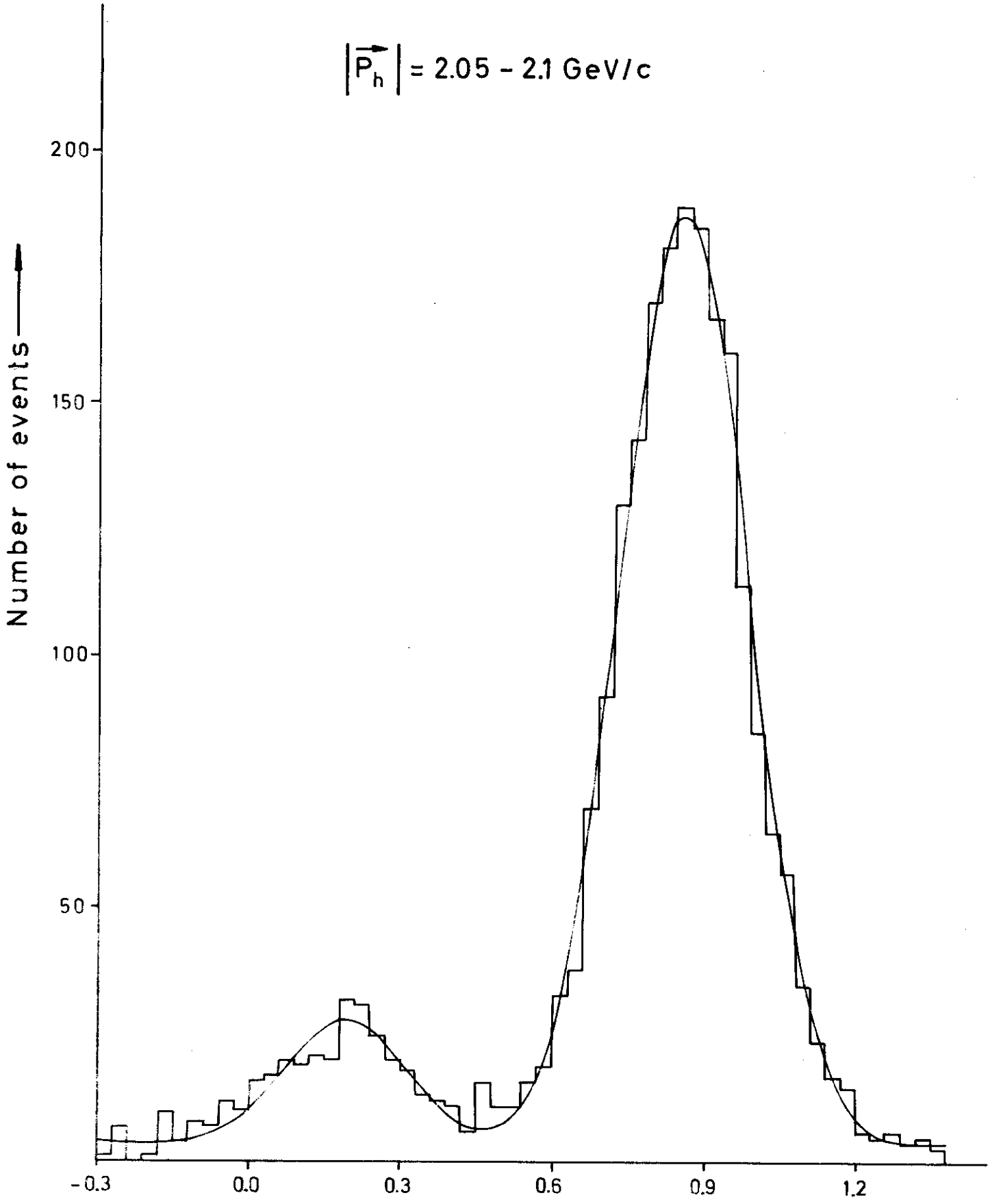
$|\vec{P_h}|$ = 2.05 - 2.1 GeV/c
Number of events
200
150
100
50
-0.3
0.0
0.3
0.6
0.9
1.2
m_h^2 [GeV^2 c^{-4}]

Fig. 3b

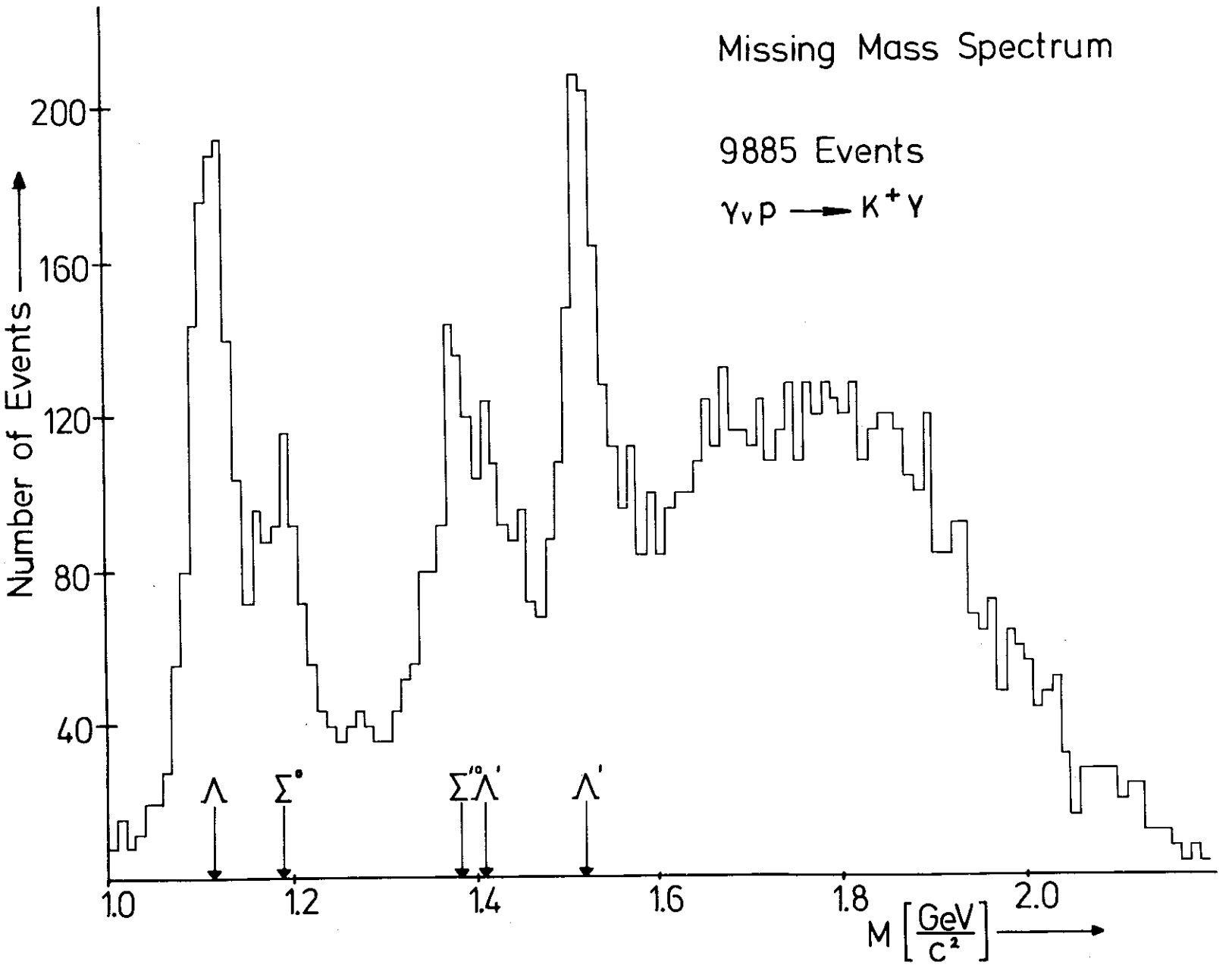
Missing Mass Spectrum
9885 Events
$\gamma_v p \rightarrow K^+ Y$
Number of Events
200
160
120
80
40
Λ
Σ^0
$\Sigma'^0\Lambda'$
Λ'
1.0
1.2
1.4
1.6
1.8
2.0
$M\left[\frac{GeV}{c^2}\right]$

Fig. 4

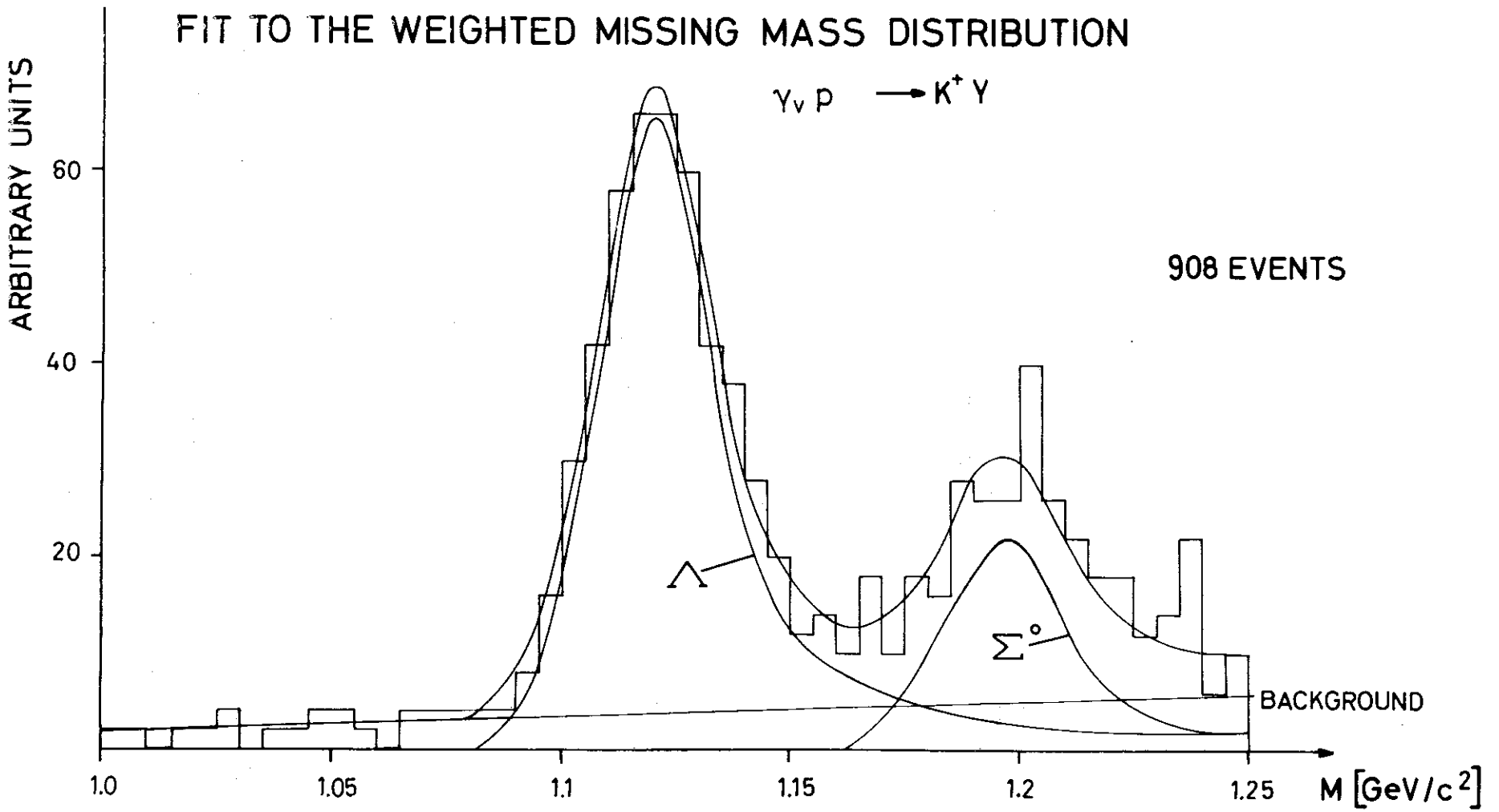
FIT TO THE WEIGHTED MISSING MASS DISTRIBUTION
$\gamma_v p \rightarrow K^+ Y$
908 EVENTS
ARBITRARY UNITS
60
40
20
Λ
Σ^0
BACKGROUND
1.0
1.05
1.1
1.15
1.2
1.25
M [GeV/c^2]

Fig. 5 a

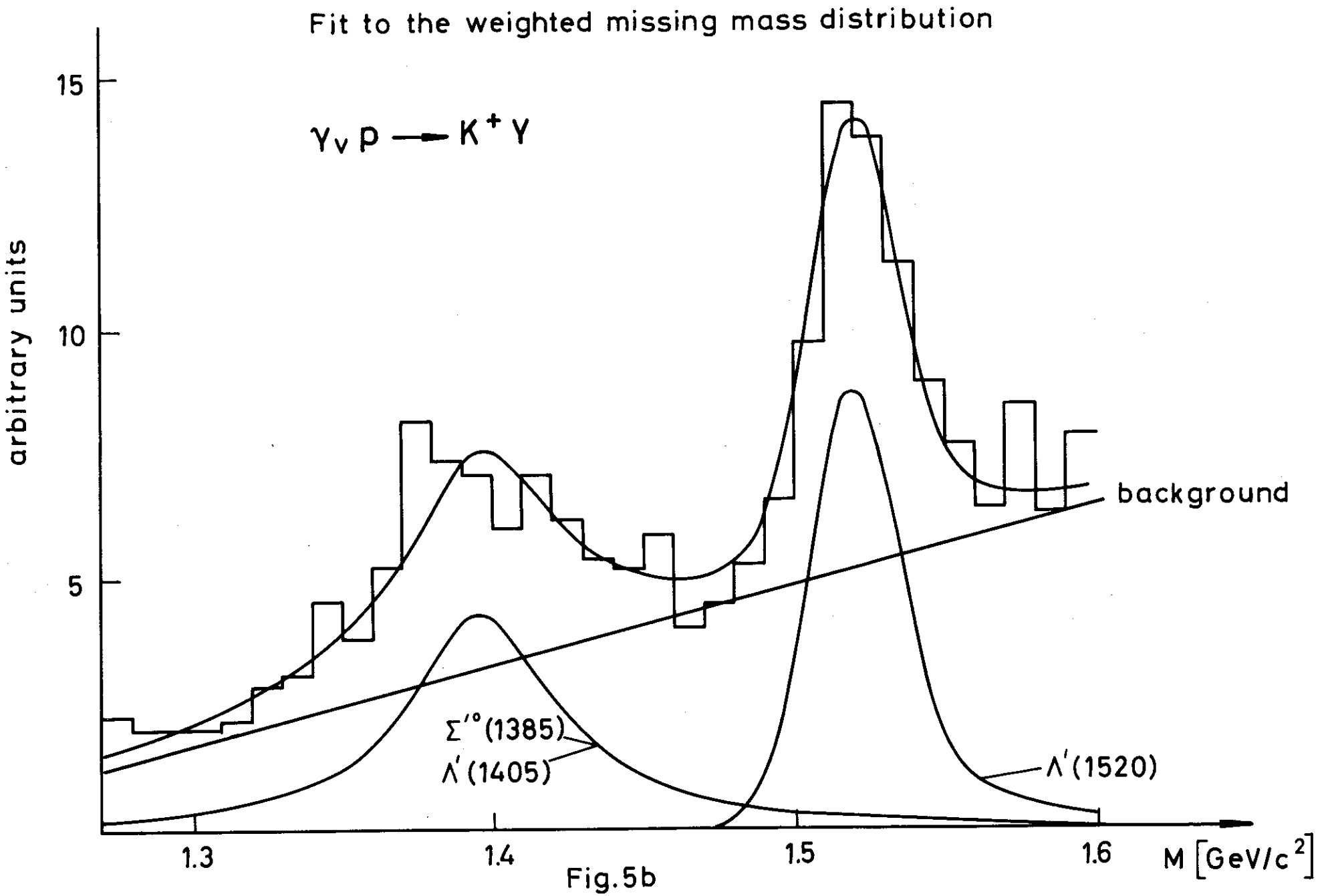
Fit to the weighted missing mass distribution
$\gamma_v p \rightarrow K^+ Y$
arbitrary units
15
10
5
background
$\Sigma'^0(1385)$
$\Lambda'(1405)$
$\Lambda'(1520)$
1.3
1.4
1.5
1.6
M [GeV/c^2]

Fig. 5b

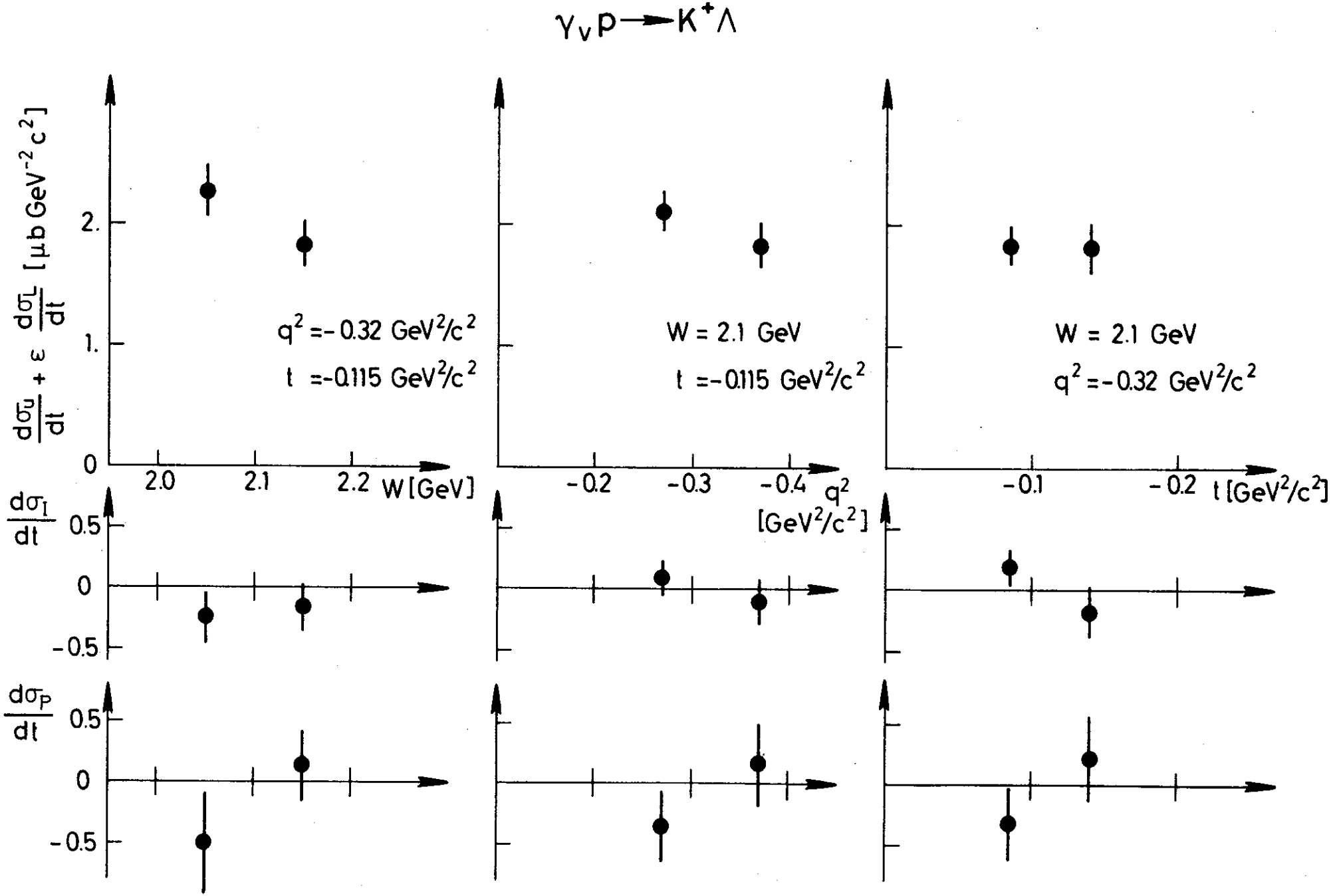
$\gamma_v p \rightarrow K^+ \Lambda$
$\frac{d\sigma_u}{dt} + \varepsilon \frac{d\sigma_L}{dt}$ [$\mu b\, GeV^{-2} c^2$]
$q^2 = -0.32\ GeV^2/c^2$
$t = -0.115\ GeV^2/c^2$
W = 2.1 GeV
$t = -0.115\ GeV^2/c^2$
W = 2.1 GeV
$q^2 = -0.32\ GeV^2/c^2$
W [GeV]
q^2 [GeV^2/c^2]
t [GeV^2/c^2]
$\frac{d\sigma_I}{dt}$
$\frac{d\sigma_P}{dt}$

Fig. 6a

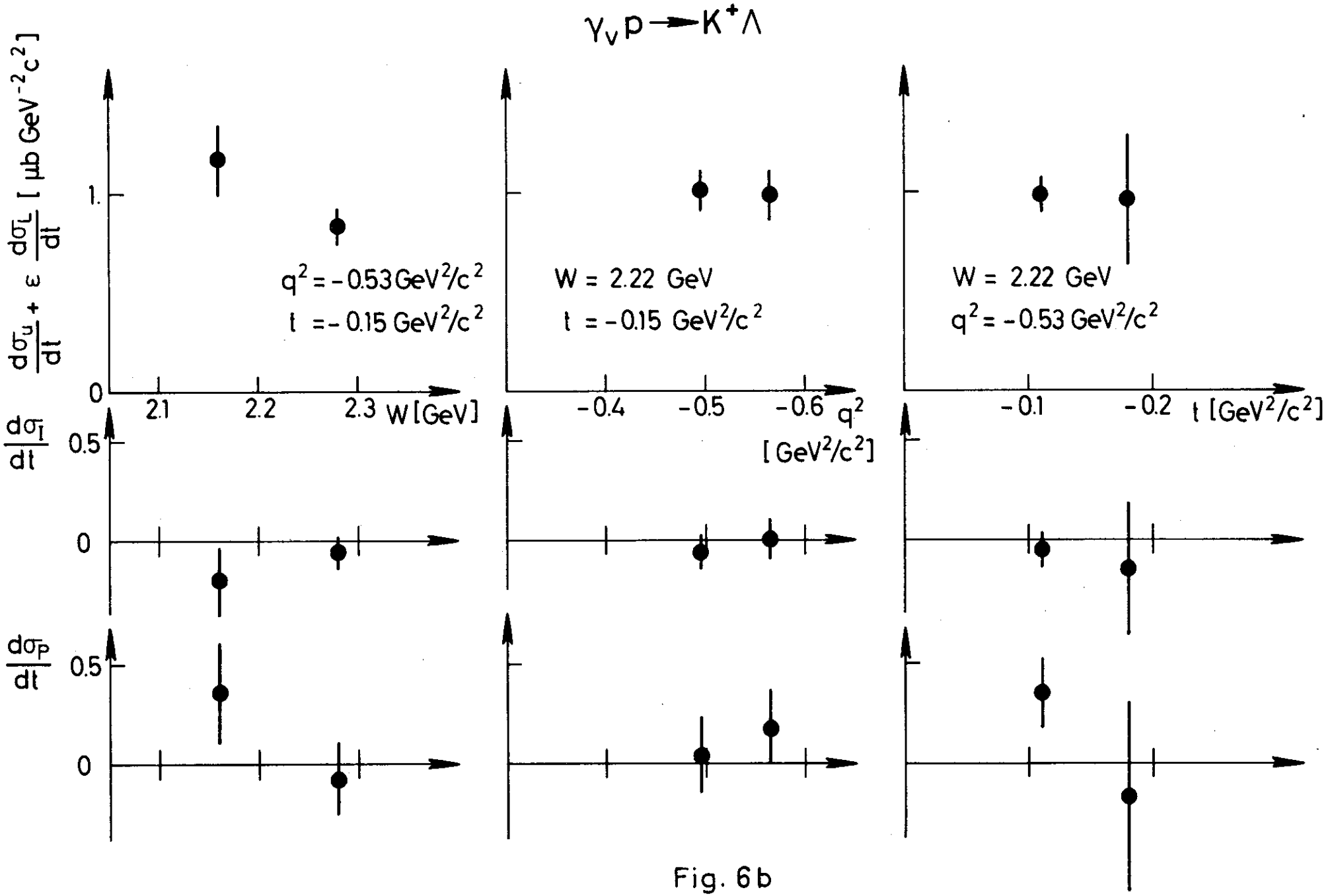
$\gamma_v p \rightarrow K^+ \Lambda$
$\frac{d\sigma_u}{dt} + \varepsilon \frac{d\sigma_L}{dt}$ [$\mu b\, GeV^{-2} c^2$]
1.
0
$q^2 = -0.53\, GeV^2/c^2$
$t = -0.15\, GeV^2/c^2$
2.1
2.2
2.3 W [GeV]
W = 2.22 GeV
$t = -0.15\, GeV^2/c^2$
-0.4
-0.5
-0.6 q^2
[GeV^2/c^2]
W = 2.22 GeV
$q^2 = -0.53\, GeV^2/c^2$
-0.1
-0.2 t [GeV^2/c^2]
$\frac{d\sigma_I}{dt}$
0.5
0
$\frac{d\sigma_P}{dt}$
0.5
0

Fig. 6b

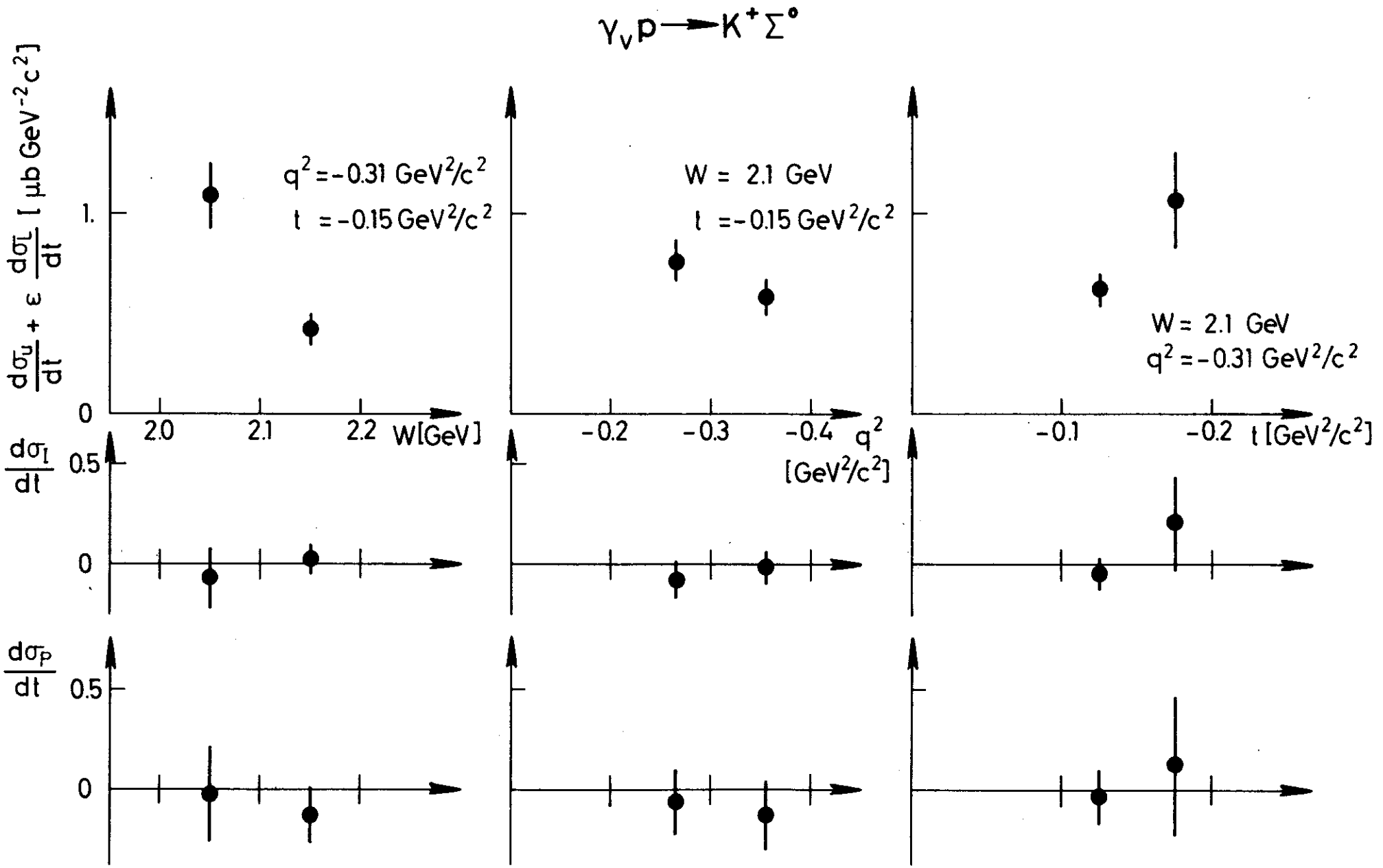
$\gamma_v p \rightarrow K^+ \Sigma^0$
$\frac{d\sigma_u}{dt} + \varepsilon \frac{d\sigma_L}{dt}$ [$\mu b\, GeV^{-2} c^2$]
$q^2 = -0.31\ GeV^2/c^2$
$t = -0.15\ GeV^2/c^2$
W = 2.1 GeV
$t = -0.15\ GeV^2/c^2$
W = 2.1 GeV
$q^2 = -0.31\ GeV^2/c^2$
1.
0
2.0
2.1
2.2
W[GeV]
-0.2
-0.3
-0.4
q^2
$[GeV^2/c^2]$
-0.1
-0.2
$t\ [GeV^2/c^2]$
$\frac{d\sigma_I}{dt}$
0.5
0
$\frac{d\sigma_P}{dt}$
0.5
0

Fig. 7a

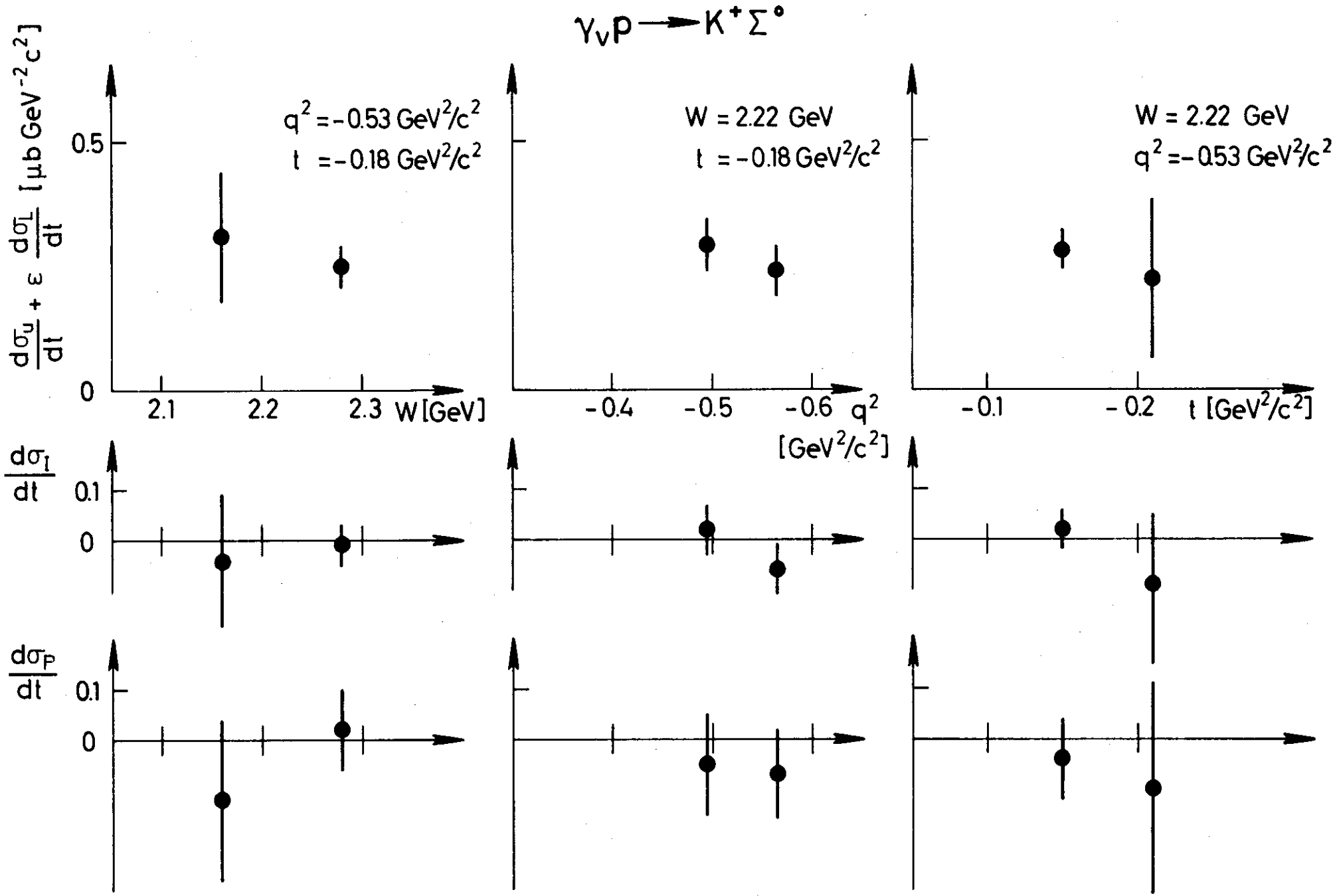
$\gamma_v p \rightarrow K^+ \Sigma^\circ$
$\frac{d\sigma_u}{dt} + \varepsilon \frac{d\sigma_L}{dt}$ [$\mu b\, GeV^{-2} c^2$]
0.5
0
$q^2 = -0.53\ GeV^2/c^2$
$t = -0.18\ GeV^2/c^2$
2.1
2.2
2.3 W [GeV]
W = 2.22 GeV
$t = -0.18\ GeV^2/c^2$
-0.4
-0.5
-0.6 q^2
[GeV^2/c^2]
W = 2.22 GeV
$q^2 = -0.53\ GeV^2/c^2$
-0.1
-0.2
t [GeV^2/c^2]
$\frac{d\sigma_I}{dt}$
0.1
0
$\frac{d\sigma_P}{dt}$
0.1
0

Fig. 7b

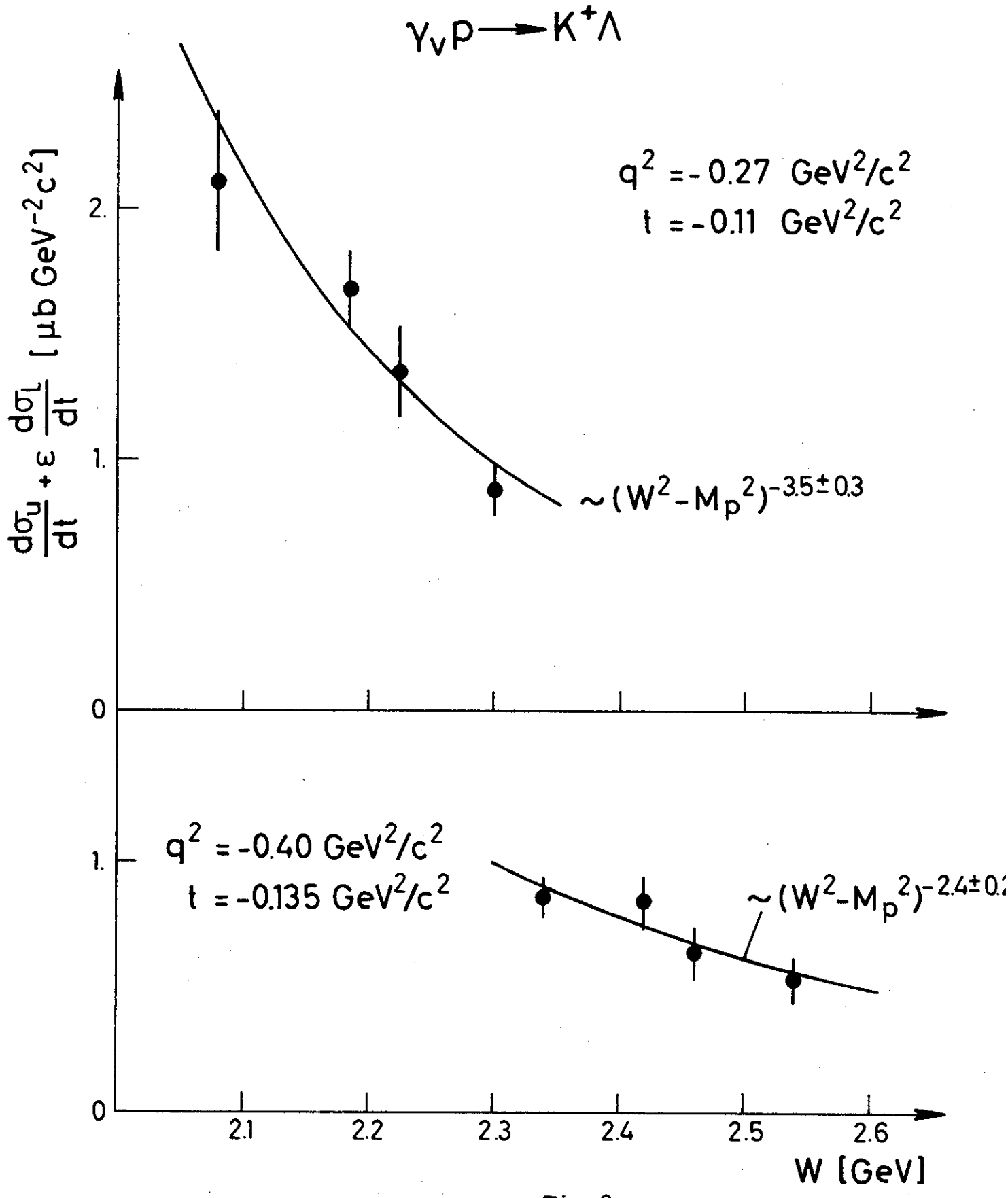
$\gamma_v p \longrightarrow K^+\Lambda$
$\frac{d\sigma_u}{dt} + \varepsilon \frac{d\sigma_L}{dt}$ [μb GeV^{-2}c^2]
$q^2 = -0.27$ GeV^2/c^2
$t = -0.11$ GeV^2/c^2
$\sim (W^2 - M_p^2)^{-3.5 \pm 0.3}$
$q^2 = -0.40$ GeV^2/c^2
$t = -0.135$ GeV^2/c^2
$\sim (W^2 - M_p^2)^{-2.4 \pm 0.2}$
2.
1.
0
1.
0
2.1
2.2
2.3
2.4
2.5
2.6
W [GeV]

Fig.8

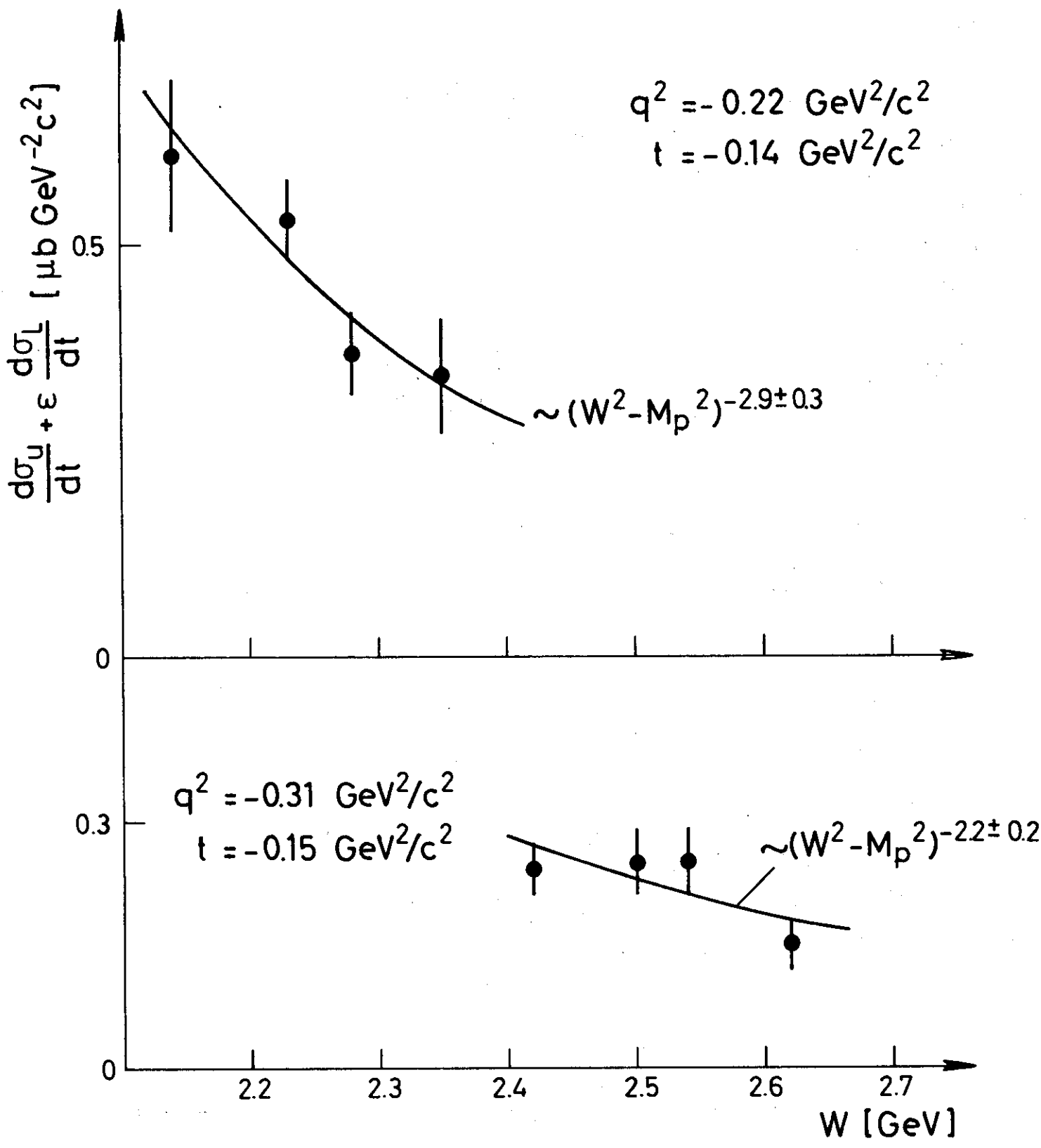
$\gamma_v p \longrightarrow K^+\Sigma^\circ$
$q^2 = -0.22$ GeV^2/c^2
$t = -0.14$ GeV^2/c^2
$\sim (W^2 - M_p^2)^{-2.9 \pm 0.3}$
$q^2 = -0.31$ GeV^2/c^2
$t = -0.15$ GeV^2/c^2
$\sim (W^2 - M_p^2)^{-2.2 \pm 0.2}$
$\frac{d\sigma_u}{dt} + \varepsilon \frac{d\sigma_L}{dt}$ [μb GeV^{-2}c^2]
0.5
0
0.3
0
2.2
2.3
2.4
2.5
2.6
2.7
W [GeV]

Fig. 9

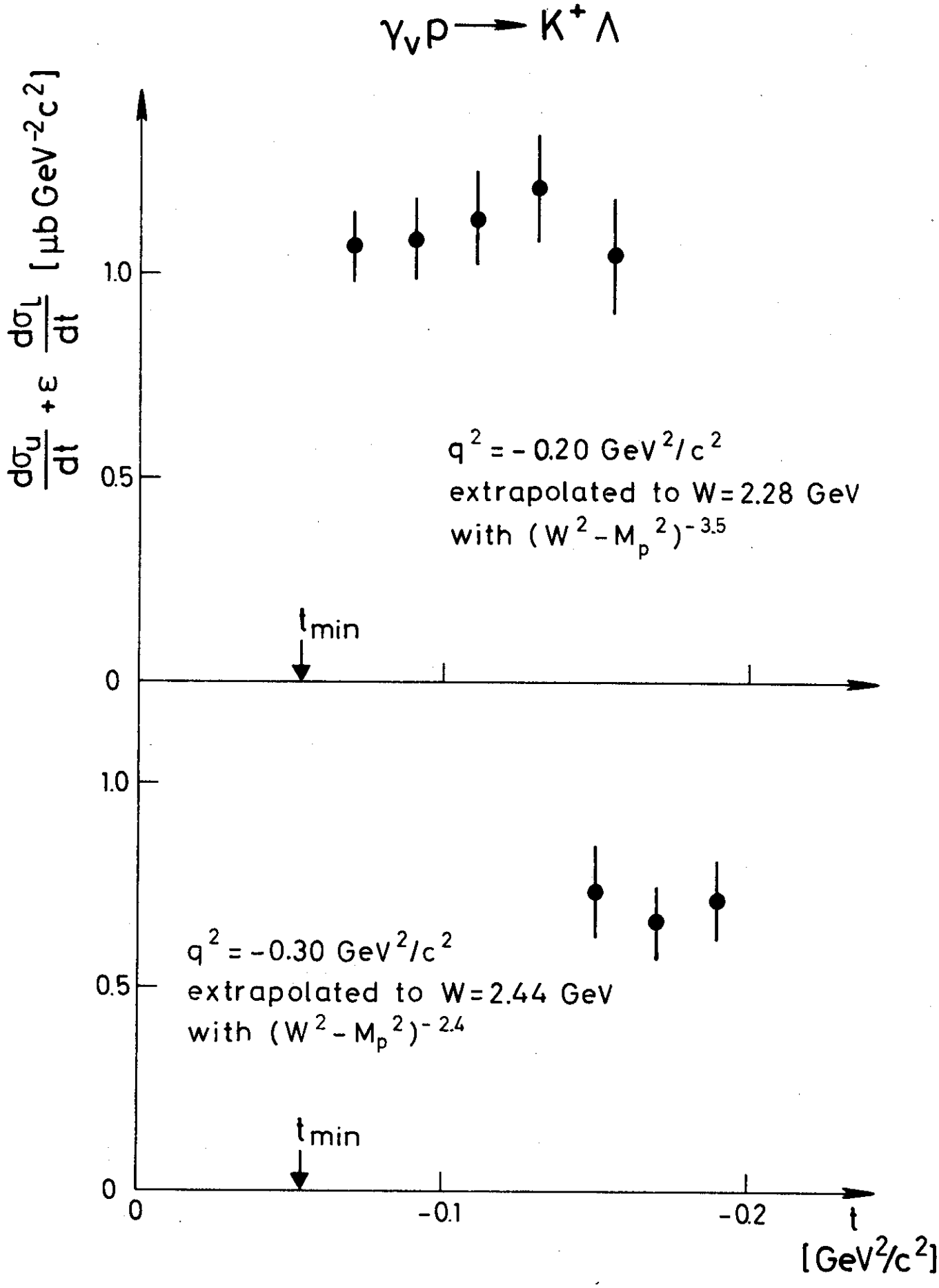
$\gamma_v p \longrightarrow K^+ \Lambda$
$\frac{d\sigma_u}{dt} + \varepsilon \frac{d\sigma_L}{dt}$ [$\mu b\, GeV^{-2} c^2$]
1.0
0.5
0
$q^2 = -0.20\ GeV^2/c^2$
extrapolated to W = 2.28 GeV
with $(W^2 - M_p^2)^{-3.5}$
t_{min}
1.0
0.5
0
$q^2 = -0.30\ GeV^2/c^2$
extrapolated to W = 2.44 GeV
with $(W^2 - M_p^2)^{-2.4}$
t_{min}
0
-0.1
-0.2
t
[GeV^2/c^2]

Fig.10

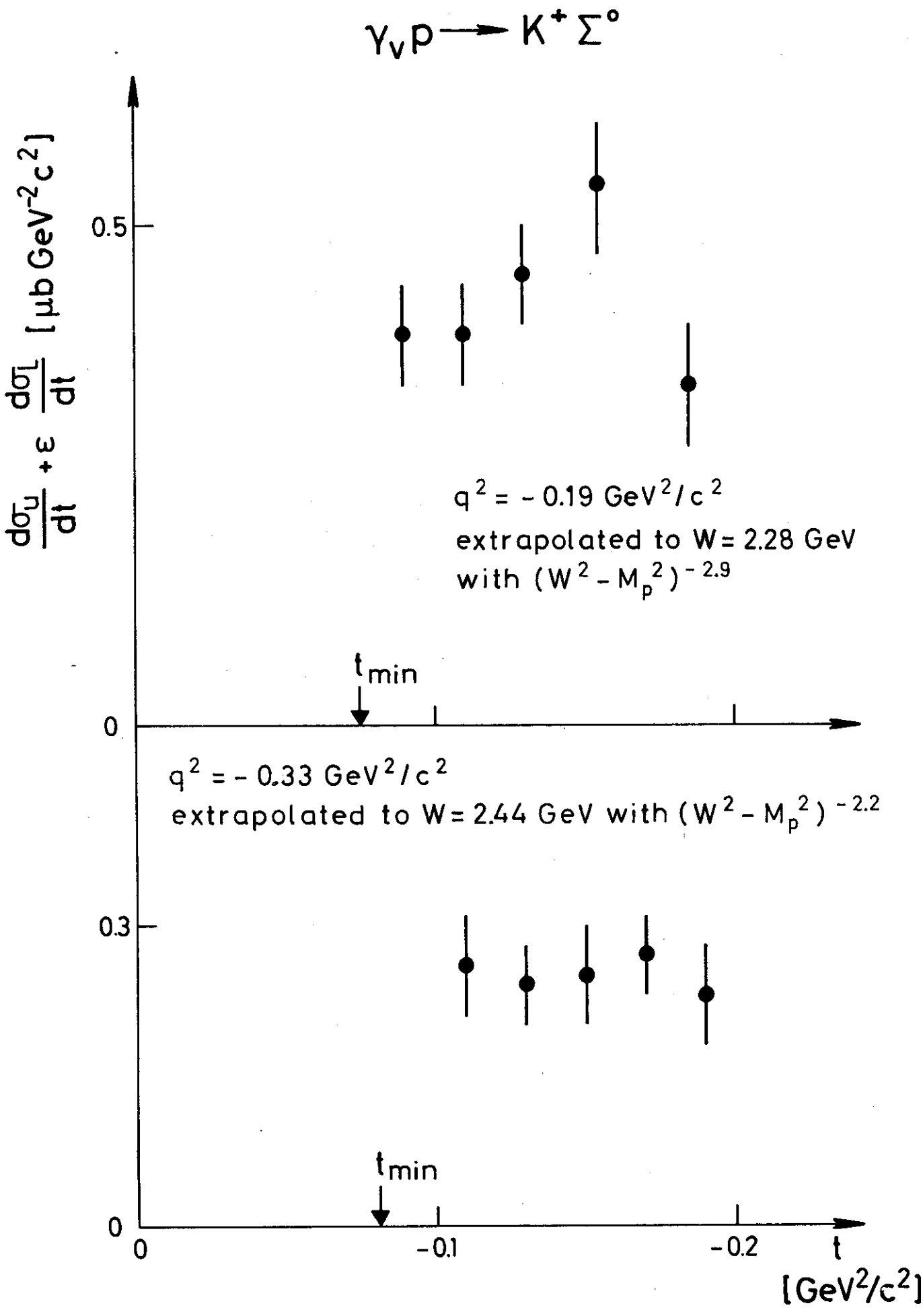
$\gamma_v p \longrightarrow K^+ \Sigma^0$
$\frac{d\sigma_U}{dt} + \varepsilon \frac{d\sigma_L}{dt}$ [$\mu b\, GeV^{-2} c^2$]
0.5
0
0.3
0
$q^2 = -0.19\ GeV^2/c^2$
extrapolated to W = 2.28 GeV
with $(W^2 - M_p^2)^{-2.9}$
t_{min}
$q^2 = -0.33\ GeV^2/c^2$
extrapolated to W = 2.44 GeV with $(W^2 - M_p^2)^{-2.2}$
t_{min}
0
-0.1
-0.2
t
[GeV^2/c^2]

Fig. 11

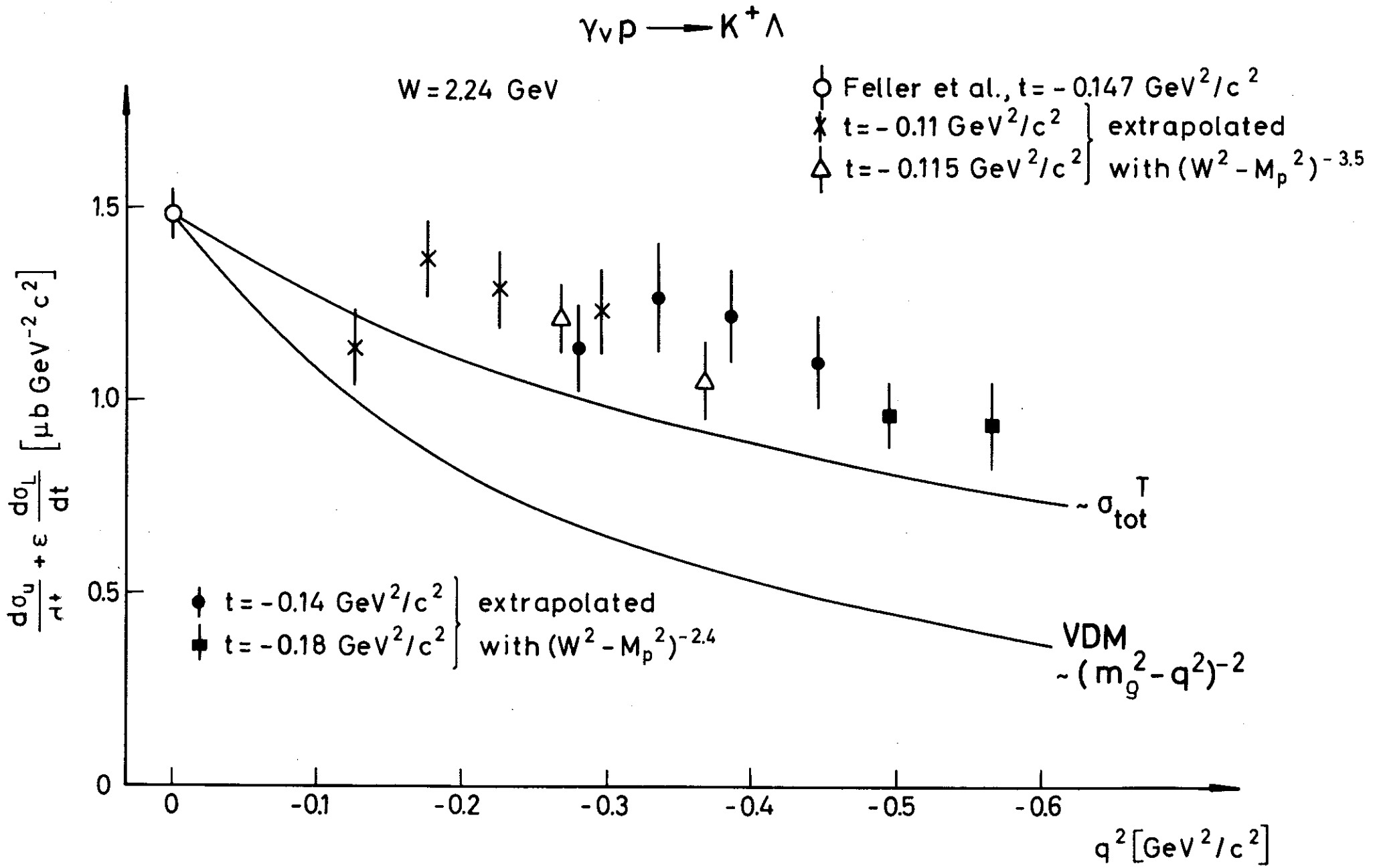
$\gamma_V p \longrightarrow K^+ \Lambda$
W = 2.24 GeV
Feller et al., t = - 0.147 GeV²/c²
t = - 0.11 GeV²/c² } extrapolated
t = - 0.115 GeV²/c² } with $(W^2 - M_p^2)^{-3.5}$
$\frac{d\sigma_u}{dt} + \varepsilon \frac{d\sigma_L}{dt}$ [μb GeV⁻² c²]
1.5
1.0
0.5
0
t = - 0.14 GeV²/c² } extrapolated
t = - 0.18 GeV²/c² } with $(W^2 - M_p^2)^{-2.4}$
$\sim \sigma_{tot}^T$
VDM
$\sim (m_g^2 - q^2)^{-2}$
0
-0.1
-0.2
-0.3
-0.4
-0.5
-0.6
q^2 [GeV²/c²]

Fig.12

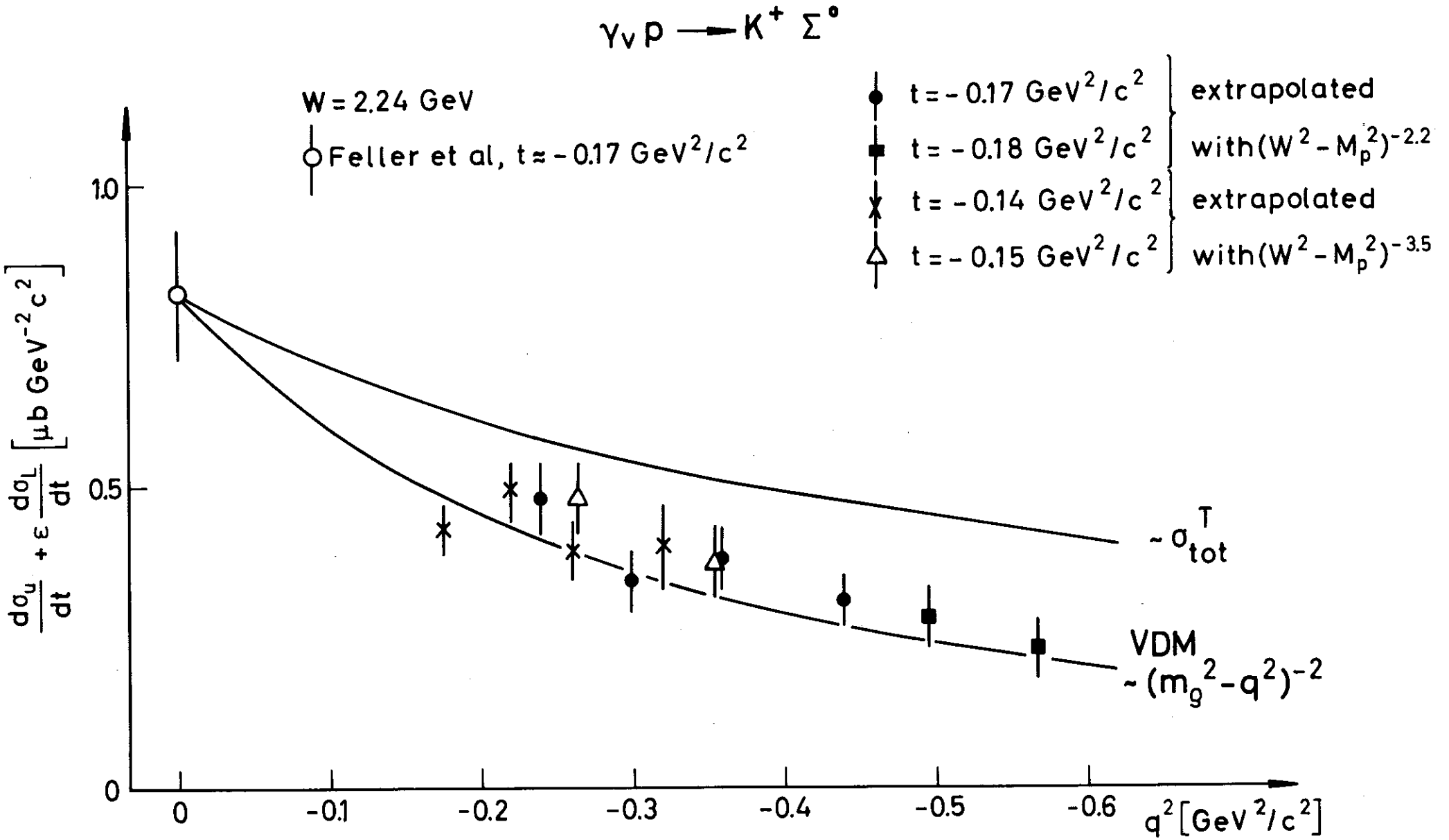
$\gamma_V p \longrightarrow K^+ \Sigma^0$
W = 2.24 GeV
Feller et al, t ≈ - 0.17 GeV²/c²
t = - 0.17 GeV²/c² } extrapolated
t = - 0.18 GeV²/c² } with $(W^2 - M_p^2)^{-2.2}$
t = - 0.14 GeV²/c² } extrapolated
t = - 0.15 GeV²/c² } with $(W^2 - M_p^2)^{-3.5}$
$\frac{d\sigma_u}{dt} + \varepsilon \frac{d\sigma_L}{dt}$ [μb GeV^{-2}c^2]
1.0
0.5
0
0
-0.1
-0.2
-0.3
-0.4
-0.5
-0.6
q^2 [GeV²/c²]
$\sim \sigma_{tot}^T$
VDM
$\sim (m_g^2 - q^2)^{-2}$

Fig.13

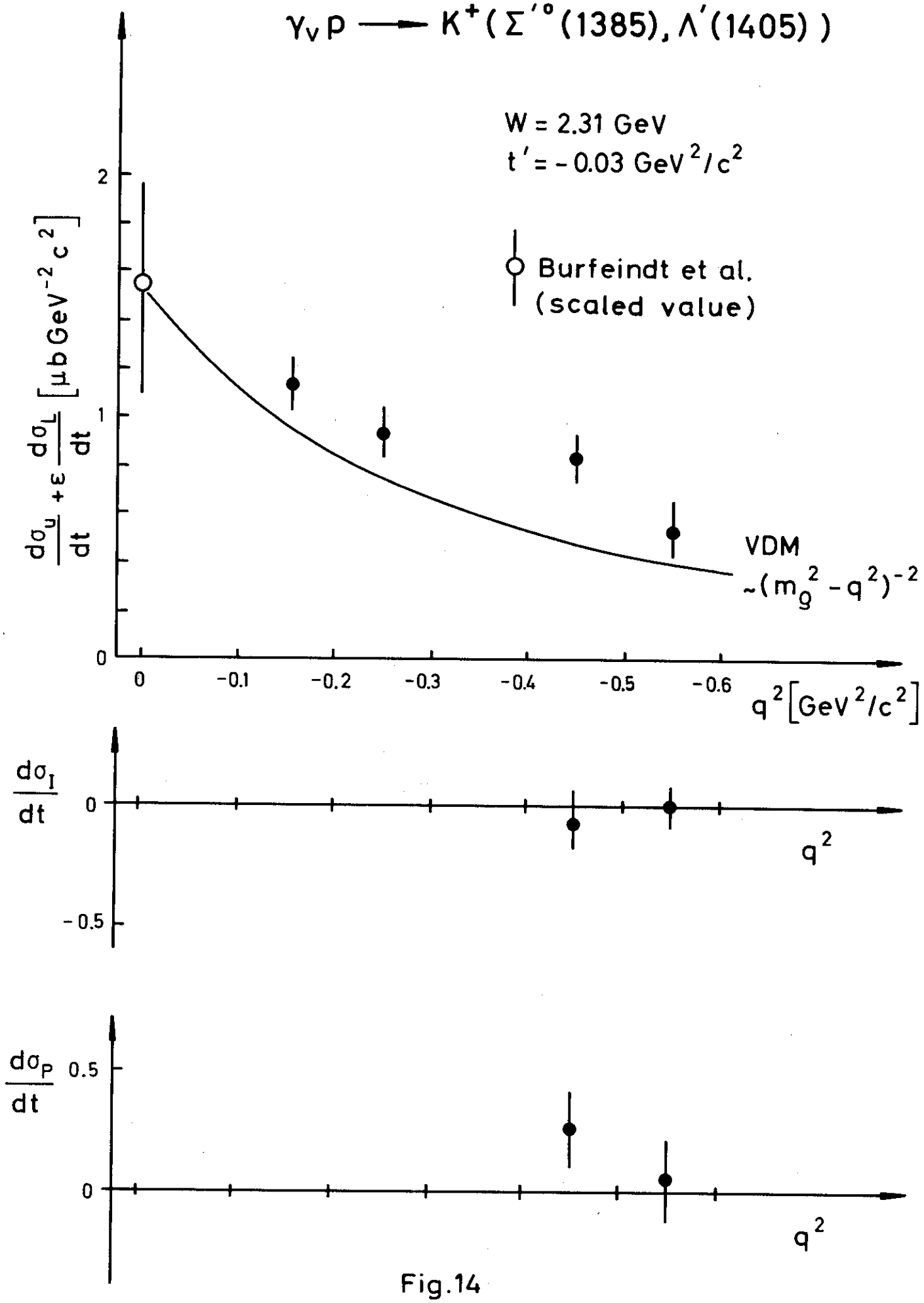
$\gamma_v p \longrightarrow K^+(\Sigma'^0(1385), \Lambda'(1405))$
W = 2.31 GeV
$t' = -0.03\ GeV^2/c^2$
Burfeindt et al.
(scaled value)
$\frac{d\sigma_u}{dt} + \varepsilon\frac{d\sigma_L}{dt}\ [\mu b\, GeV^{-2} c^2]$
VDM
$\sim(m_\varrho^2 - q^2)^{-2}$
$q^2[GeV^2/c^2]$
$\frac{d\sigma_I}{dt}$
$\frac{d\sigma_P}{dt}$
q^2

Fig.14

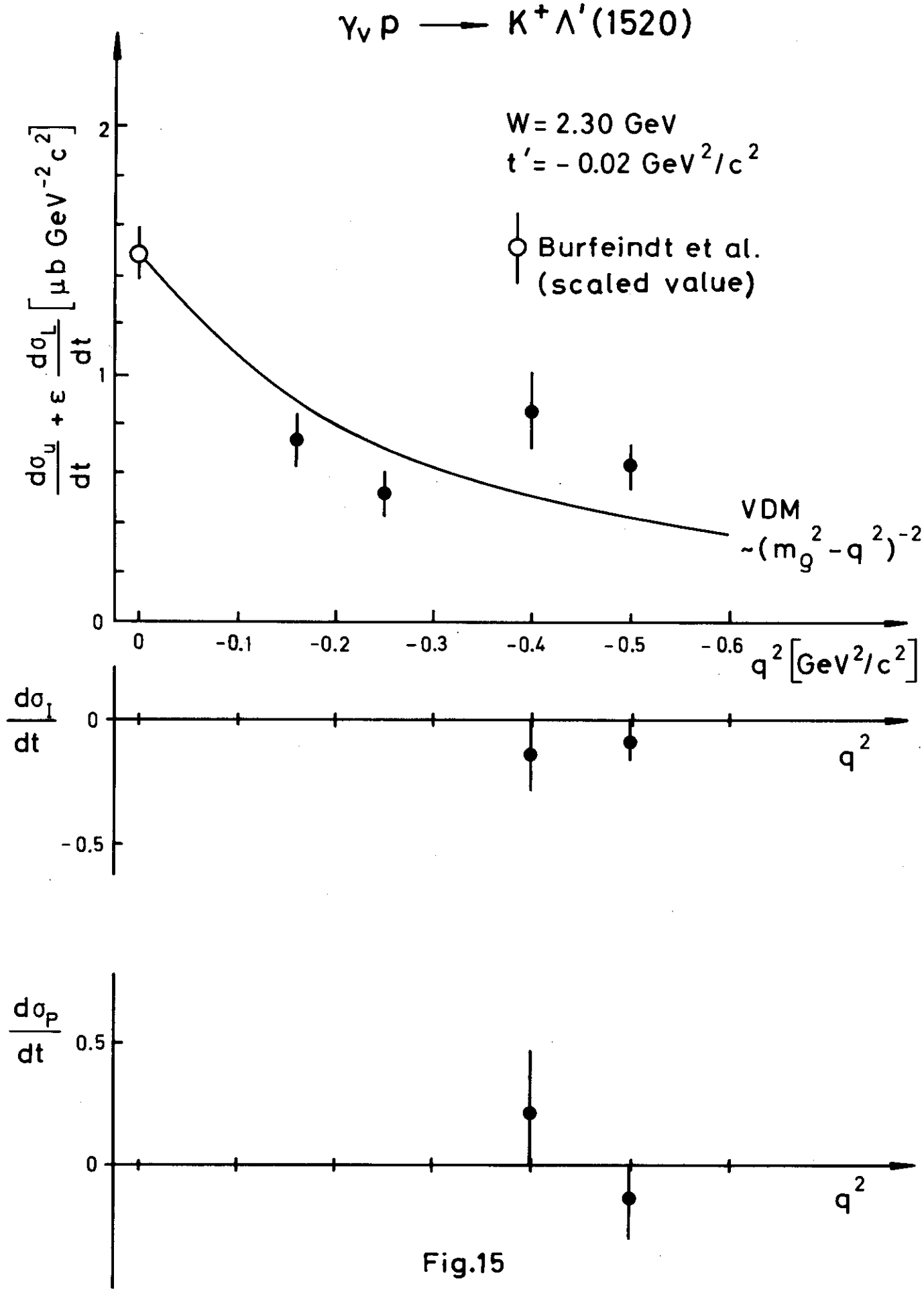
$\gamma_v p \longrightarrow K^+ \Lambda'(1520)$
W = 2.30 GeV
$t' = -0.02\ GeV^2/c^2$
Burfeindt et al.
(scaled value)
$\frac{d\sigma_u}{dt} + \varepsilon \frac{d\sigma_L}{dt} \left[\mu b\ GeV^{-2} c^2\right]$
VDM
$\sim (m_\varrho^2 - q^2)^{-2}$
$q^2 \left[GeV^2/c^2\right]$
$\frac{d\sigma_T}{dt}$
$\frac{d\sigma_P}{dt}$
q^2

Fig.15